UNIVERSITY OF NAPLES FEDERICO II

DEPARTMENT OF VETERINARY MEDICINE AND PRODUCTION OF ANIMALS

DOCTORATE IN VETERINARY SCIENCE

CYCLE XXXV

Reactivation of the Retinoblastoma family of proteins by Cyclin-dependent kinase inhibitors in Canine Mammary Tumors

Coordinator: Prof. Paolo De Girolamo

Supervisor: Prof. Luigi Avallone

Cosupervisor: Prof.ssa Francesca Ciani

Ph.D. degree thesis of:

Asadoor Amirkhani Namagerdi

Academic year 2022-2023

Contents

Abstract

Comparative Oncology refers to the discipline that integrates the naturally occurring cancers seen in veterinary patients into more general studies of cancer biology and therapy. This includes the study of cancer pathogenesis (i.e., the study of cancer-associated genes and proteins) and the study of new treatment options for the management of cancer. This approach provides novel opportunities for current and future veterinary and human cancer patients. Although several veterinary species, including cats, horse, and ferret, develop cancers that are of comparative interest, the majority of both the scientific and clinical effort has thus far focused on the dog.

The partially overlapping transcriptome and proteome of metastatic canine mammary tumors (CMT) and human breast cancer (HBC) suggests that there are underlying comparable evidence that metastatic canine carcinomas are suitable translational model for human breast tumors which could be used to determine prognostic and predictive molecular signatures and identify therapeutic targets. The retinoblastoma tumor suppressor (RB) protein is functionally inactivated in many human cancers and is aberrant in one-third of all breast cancers. RB regulates G1/S-phase cell-cycle progression and is a critical mediator of antiproliferative signaling. It is known that pRb can be inactivated by various mechanisms including genetic mutations and phosphorylation. The most important target of the retinoblastoma (RB) protein family members (p105, p107 and p130) is the E2F-family of transcription factors, which control the expression of genes that mediate G1-S transition. Together, these proteins are often referred to as the pocket proteins. At the transition to S-phase, cyclin/CDK complexes phosphorylate the pocket proteins and transcription of E2F target genes proceeds through S phase. Cell-cycle progression is mediated by cyclin-dependent kinases (CDKs) and their regulatory cyclin subunits. Overexpression and/or dysfunction of CDKs or cyclins have been reported in a very large number of human cancers and other diverse pathologies. These protein kinases are considered as valuable therapeutic targets for drug development. CDK4/6 inhibitors like palbociclib inhibit CDK4/6-mediated phosphorylation of RB.

In this study we showed that Palbociclib inhibits pRb phosphorylation in the CMT primary cells that express CDK4, CDK6 and Rb family of proteins independent of ER expression, in a dose and time dependent manner. Moreover, it decreased CMT cells migration, spheroid formation and colony formation. Our findings suggest that palbociclib as a CDK4/6 inhibitor can be a candidate for the treatment of CMTs.

Reactivation of the Retinoblastoma family of proteins by Cyclin-dependent kinase (CDK) inhibitors in Canine Mammary Tumors (CMT)

Introduction:

Canine Mammary Tumors

Cancer constitutes the major health problem both in human and veterinary medicine. Comparative oncology as an integrative approach offers to learn more about naturally occurring cancers across varied species. It integrates the naturally occurring cancers seen in the veterinary patients into more general studies of cancer biology and therapy. This includes the study of cancer pathogenesis (i.e., the study of cancer-associated genes and proteins) and the study of new treatment options for the management of cancer. By nature, this approach provides novel opportunities for current and future veterinary and human cancer patients. Although several veterinary species, including the cat, horse, and ferret, develop cancers that are of comparative interest, the majority of both the scientific and clinical effort has thus far focused on the dog[1].

Canine models have many advantages as they experience spontaneous disease, have many genes like human genes, five to seven-fold accelerated ageing compared to humans, respond to treatments similarly as humans do and health care levels second only to humans[2]. The shorter lifespan of dogs compared to humans enables researchers to study cancers that develop after a few years instead of decades, a time course that is sufficient to allow comparison of treatment responses while still being short enough to ensure rapid conclusion of the clinical trials[3]. With the revealing of the dog genome in 2005 and, the cat genome in 2014, the study of spontaneous cancers in these animals has become even more interesting for comparative oncology[4]. During the last few years, along with the sequencing of the entire dog genome (99% complete, ~2.5 billion base pairs) and the clear evidence of its close similarity with the human genome, the dog has emerged as an attractive alternative model for cancer research[5].

Canine mammary tumors (CMTs) are a naturally occurring heterogenous group of cancers that have several features in common with human breast cancer (HBC). These similarities include etiology, signaling pathway activation and histological classification[3].

CMTs represent between 50 and 70% of all tumors in intact female dogs. The prevalence varies depending on the geographic location, being greater in countries where ovariectomy is not routinely performed. In these countries, the prevalence of mammary neoplasms in female dogs is three times higher than the prevalence in women[6]. Data retrieved from the Animal Tumor registry of dogs and cats of Venice and Vicenza provinces during 2005-2013 by Vascellari et al.[7] showed that 54% of 2744 mammary tumors were in female dogs with an annual incidence rate was 250 cases per 100,000 dogs. The most frequent malignant CMTs were complex carcinomas, consisting of both epithelial and myoepithelial tissues, and simple carcinomas. CMTs usually affects middle-aged and older dogs with an increased risk between 8–11 years old. Benign tumors are more likely in dogs ranging between 7 and 9 years, while malignant tumors are more frequently encountered in older dogs. However, the peak incidence dictated by the age should be carefully evaluated given that larger breeds of dogs have a naturally shorter lifespan and therefore tend to be younger than smaller breeds when they receive a cancer diagnosis.

Mammary neoplasm can occur in dogs of any breed, although pure breeds seem more prone to develop CMTs. Poodles, Chihuahuas, Dachshunds, Yorkshire Terriers, Maltese, and Cocker Spaniels are frequently listed as high-risk dog breeds in the small breed category. Some of the larger breeds are also at higher risk, including the English Springer Spaniel, English Setters, Brittany Spaniels, German Shepherds, Pointers, Doberman Pinschers, and Boxers[8].

The partially overlapping transcriptome and proteome of metastatic CMT and HBC suggests that there are underlying comparable evidence that metastatic canine carcinomas are suitable translational model for human breast tumors and could be used to determine prognostic and predictive molecular signatures and identify therapeutic targets[3].

Histologic classification

In humans invasive ductal carcinomas of not otherwise specified (NOS) is the predominant histologic subtype within all the patient populations, with invasive lobular carcinoma being the subsequent predominant histologic subtype[9]. For CMTs in 2011, Goldschmidt et al.[10] proposed a new comprehensive histological classification based on the CMT classifications previously published by the World Health Organization in 1974

and 1999. Histologically, CMTs are classified as malignant epithelial neoplasms, malignant epithelial neoplasms of special types (Squamous cell carcinoma, Adenosquamous carcinoma, Mucinous carcinoma, Lipid-rich (secretory) carcinoma, Spindle cell carcinoma, and inflammatory carcinoma), malignant mesenchymal neoplasms, carcinosarcoma, benign neoplasms, Hyperplasia/Dysplasia, Neoplasms of the Nipple, and Hyperplasia/Dysplasia of the Nipple[11]. Canine mammary malignant epithelial neoplasms by themselves include Carcinoma–in situ, Carcinoma–simple (Tubular, Tubulo-papillary, Cystic-papillary, Cribriform), Carcinoma–micropapillary invasive, Carcinoma–solid, Comedocarcinoma, Carcinoma–anaplastic, Carcinoma arising in a complex adenoma/mixed tumor, Carcinoma–complex type, Carcinoma and malignant myoepithelioma, Carcinoma–mixed type, Ductal carcinoma–malignant counterpart of ductal adenoma, Intraductal papillary carcinoma–malignant counterpart of intraductal papillary adenoma[11] (diagram 1 and figure 1[10]).

Diagram 1- Goldschmidt et al.[10] proposed histological classification of canine mammary tumors (CMT) subtypes.

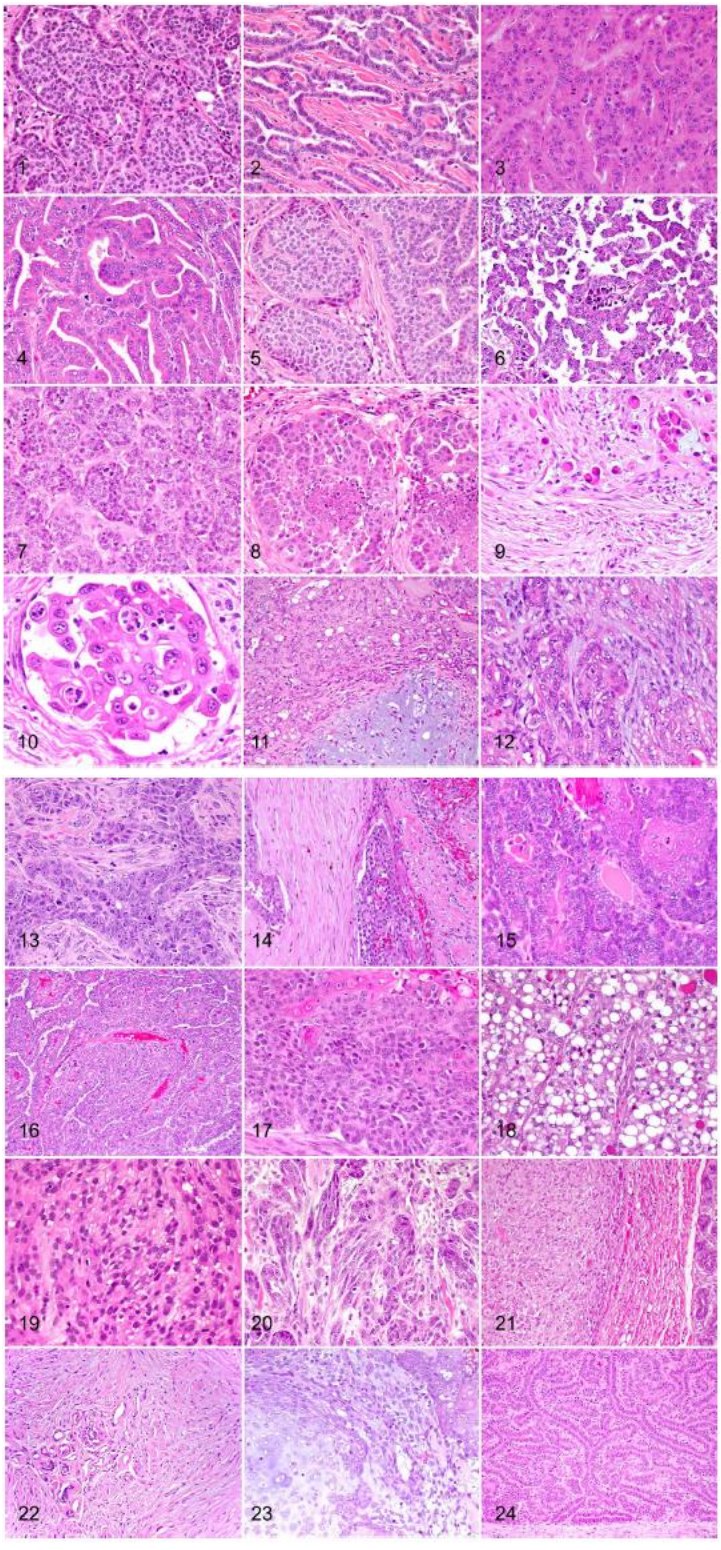
1
2
3
4
5
6
7
8
9
10
11
12
13
14
15
16
17
18
19
20
21
22
23
24

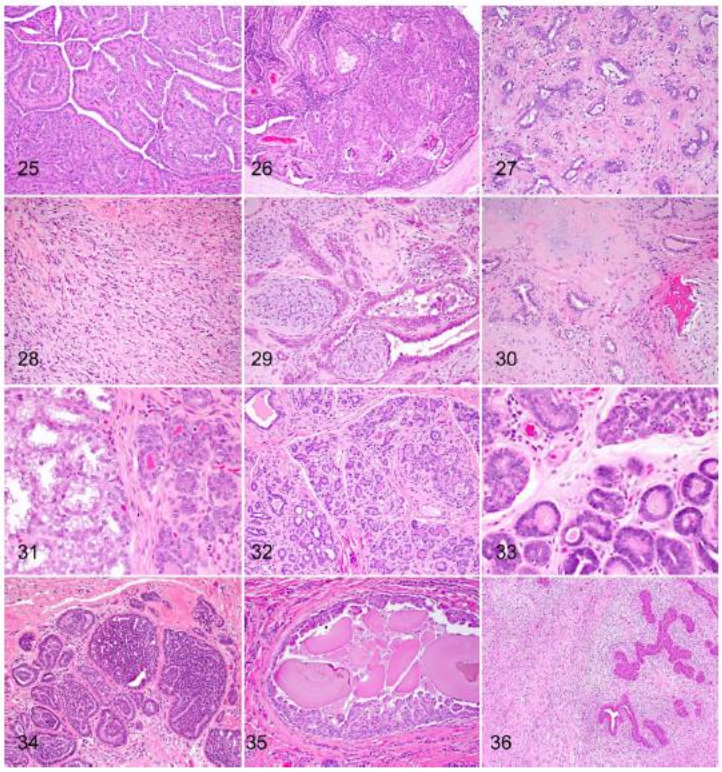

Figure 1- 1. Carcinoma in situ, mammary gland, canine. The neoplastic cells, arranged in tubules, are surrounded by an intact basement membrane. There is mild cellular and nuclear pleomorphism and occasional mitoses. HE. 2. Carcinoma, tubular type with interlobular fibrosis, mammary gland, canine. There is mild cellular and nuclear pleomorphism (lower grade). HE. 3. Carcinoma tubular type with considerable nuclear and cellular pleomorphism and frequent mitoses, mammary gland, canine (higher grade). HE. 4. Carcinoma, tubulopapillary type, with moderate nuclear and cellular pleomorphism, mammary gland, canine. The papillae are supported by a fine fibrovascular stroma. HE. 5. Carcinoma, cribriform type, mammary gland, canine. The ducts are filled with a uniform population of cells that surround small lumina. HE. 6. Carcinoma, micropapillary type, mammary gland, canine. The papillae are seen as small intraluminal aggregates of cells without a supporting stroma. HE. 7. Carcinoma, solid type, mammary gland, canine. The cells have hyperchromatic nuclei and little cytoplasm and form lobules without tubular differentiation. HE. 8. Comedocarcinoma, mammary gland, canine. Note the central area of necrosis, whereas the peripheral neoplastic cells are viable. HE. 9. Anaplastic carcinoma with desmoplasia, mammary gland, canine. The neoplastic. cells are seen as single cells or small nests of cells surrounded by marked desmoplasia. HE. 10. Anaplastic carcinoma, intralymphatic with vasculogenic mimicry, mammary gland, canine. HE. 11. Carcinoma arising in a benign mixed mammary tumor, mammary gland, canine. The chondroid component is benign, but there is moderate nuclear pleomorphism of the epithelial cells. HE. 12. Complex carcinoma, mammary gland, canine. There is pleomorphism of the epithelial cells that line the tubules but not the fusiform myoepithelial cells. HE. 13. Carcinoma and malignant myoepithelioma, mammary gland, canine. Both the epithelial cells and the myoepithelial cells are pleomorphic. HE. 14. Carcinoma–mixed type, mammary gland, canine. The malignant epithelial component forms tubules, and the mesenchymal component consists of islands of bone. The myoepithelial component is not shown. HE. 15. Ductal carcinoma, mammary gland, canine. The ducts are lined by a bilayered epithelium with foci of squamous differentiation and intracytoplasmic keratohyaline granules. HE. 16. Intraductal papillary carcinoma, mammary gland, canine. The neoplastic cells exhibit considerable nuclear and cellular pleomorphism. HE. 17. Adenosquamous carcinoma, mammary gland, canine. There is a single cells or small groups of cells showing squamous differentiation. HE. 18. Lipid-rich carcinoma, mammary gland, canine. The nuclei are at the periphery of the cell with a single large lipid vacuole or several small lipid vacuoles within the cytoplasm. HE. 19. Malignant myoepithelioma, mammary gland, canine. The cells are fusiform and have an eosinophilic cytoplasm. There is moderate nuclear and cellular pleomorphism. HE.

20. Carcinoma–spindle cell variant, mammary gland, canine. Note the intimate association of the neoplastic spindle cells with the islands of tubular epithelium. HE. 21. Osteosarcoma, mammary gland, canine. Islands of tumor osteoid are present with the neoplasm. The adjacent mammary glands exhibit lobular hyperplasia. HE. 22. Fibrosarcoma, mammary gland, canine. The remnants of mammary ducts are surrounded by the neoplastic spindle cells. HE. 23. Malignant mixed mammary tumor (carcinosarcoma), mammary gland, canine. Two neoplastic populations are present. There are neoplastic cells showing chondroid differentiation (chondrosarcoma) and islands of carcinoma cells. HE. 24. Adenoma, mammary gland, canine. The ducts are lined by a uniform population of columnar cells. HE. 25. Intraductal papillary adenoma, mammary gland, canine. The papillae are covered by a uniform population of cuboidal epithelial cells, and in the fibrovascular supporting stroma are normal myoepithelial cells. HE. 26. Ductal adenoma, mammary gland, canine. The duct lumina are lined by a double layer of epithelial cells with several foci of squamous differentiation. HE. 27. Fibroadenoma, mammary gland, canine. The ducts are surrounded by an extensive fibrous stroma. HE. 28. Myoepithelioma, mammary gland, canine. The spindled myoepithelial cells are surrounded by a mucinous and collagenous matrix. HE. 29. Complex adenoma (adenomyoepithelioma), mammary gland, canine. There are foci of myoepithelial cell proliferation adjacent to several ducts. The myoepithelial cells are fusiform to stellate and surrounded by a basophilic mucinous matrix. HE. 30. Benign mixed tumor, mammary gland, canine. Note the ductal and myoepithelial cells with foci of chondroid and osseous differentiation. HE. 31. Lobular hyperplasia with lactation, mammary gland, canine. The lactational changes are characterized by cells with a vacuolated cytoplasm. HE. 32. Lobular hyperplasia with fibrosis, mammary gland, canine. Note the extensive intralobular fibrosis. HE. 33. Lobular hyperplasia with atypia, mammary gland, canine. The nuclei are hyperchromatic with an increased nuclear:cytoplasmic ratio. In some ducts, there is piling up of the epithelium. HE. 34. Epitheliosis, mammary gland, canine. The intraductal proliferation is by cells with chromatic nuclei. These cells are smaller than the peripheral ductal epithelial cells. HE. 35. Duct papillomatosis, mammary gland, canine. Multifocal intraluminal papillary proliferation without any supporting stroma and several corpora amylacea. HE. 36. Fibroadenomatous change, mammary gland, canine. There is proliferation of the interlobular ducts and extensive proliferation of the edematous interlobular stroma. HE.

The gross morphology of 26 cases of CMTs was studied by Patel et al.[12]. The weight of the tumors varied from 30 to 2000 grams and most of them were round to oval with a soft to hard consistency and a grayish-white cut surface. Of the 229 CMT tumors studied by Goldschmidt et al.[10], 169 (74%) were malignant and 60 (26%) were benign. Among the malignant tumors, complex carcinoma was the most common (13.6%), followed by carcinoma and malignant myoepithelioma (11.8%), solid carcinoma (11.8%), anaplastic carcinoma (10.6%), comedocarcinoma (10%), simple tubular carcinoma (8.9%), carcinoma arising in benign mixed tumor (8.3%), simple tubulopapillary carcinoma (7.1%), intraductal papillary carcinoma (7.1%), adenosquamous carcinoma (5.9%), and carcinosarcoma (4.7%). Myoepithelial cell proliferation is much more common, occurring in more than 20% of CMTs compared to less than 0.1% in HBCs. Canine simple carcinomas have no myoepithelial cell proliferation, while canine complex carcinomas have both proliferating luminal and myoepithelial cells. Histologically, canine simple carcinomas mirror human breast carcinomas[13].

Molecular Classification

Sørlie et al.[14] by using gene expression profiling (GEP) on 456cDNA clones of the breast, classified human breast cancers into five intrinsic subtypes, i.e., luminal A (ER+, PR+, HER2-, KI67-), luminal B (ER+, PR+, HER2+/-, KI67+), HER2 over-expression (ER-, PR-, HER2+), basal-like (ER-, PR-, HER2-, CK5/6+) and normal-like tumors (ER+, PR+, HER2-, KI67-).

Normal-like and luminal A tumors have the same immunohistochemistry features but differ on expression pattern[15]. Some studies show that normal-like may be an artifact of contamination of tumor RNA with RNA from normal breast cells[16] and normal-like breast cancer subtype is now less frequently used[17] (Table 1). In 2007, Herschkowitz et al.[18] identified a new molecular subtype, referred to as claudin-low.

Despite the apparent similarity to basal-like tumors, Prat et al.[19] showed that claudin-low tumors as a group did not show high expression of proliferation genes and thus are likely slower-cycling tumors. Clinically, most claudin-low tumors are estrogen receptor (ER)-negative, progesterone receptor (PR)-negative, and epidermal growth factor receptor 2 (HER2)-negative (triple-negative) with poor prognosis. TNBCs and basal-like breast cancers were previously thought to be the same but transcriptomic analyses have shown that TNBCs are highly heterogenous[20]. Not all triple negative (TN) tumors are identified as basal-like by gene expression, and not all basal-like tumors are TN[21].

In the largest canine mammary cancer cohort reported by Abadie et al.[22] 350 female canine mammary cancers were classified as luminal A (14.3%), luminal B (9.4%), no HER2-overexpressing and triple negative (76.3%) either of the basal-like type (ER- and PR-, EGFR and/or CK5/6+) (58.6%) or of the non-basal-like type (ER- and PR-, EGFR, and CK5/6-) (17.7%)[22]. Im et al.[23] showed that Carcinoma-tubular and carcinoma arising in a complex adenoma/mixed tumor were frequently categorized as luminal A, whereas carcinoma-solid was frequently categorized as basal-like.

Dogs are therefore powerful spontaneous models of cancer to test new therapeutic approaches, particularly for human triple-negative breast cancers.

TABLE 1- Intrinsic subtypes of breast cancer by Sørlie et al.[14]

Intrinsic subtype	**IHC status**
Luminal A	ER+, PR+, HER2-, KI67-
Luminal B	ER+, PR+, HER2+/-, KI67+
HER2 over-expression	ER-, PR-, HER2+
Basal-like	ER-, PR-, HER2-, CK5/6+

Genetics and epigenetics

In HBC, genes with at least a fourfold rise in pathogenic mutations compared with unaffected controls are usually categorized as high-risk BC genes. These include BRCA1/2, CDH1, PALB2, PTEN, STK11, and TP53[24]. While germline BRCA1/2 mutations occur in 5.3% of unselected HBC according to The Cancer Genome Atlas (TCGA), a recent study showed that 11.2% of unselected TNBC cases had deletions in the BRCA1 (8.5%) and BRCA2 (2.7%) respectively[25]. About 70% of breast cancers in BRCA1 mutation carriers and up to 23% of BRCA2 carriers are triple-negative[26].

The somatic mutation landscape of human TNBC shows the highest frequency of TP53 mutations, up to 80%[27]. Shah et al.[28] sequenced 104 TNBC tumors and found that the most common mutation was TP53 (53.8%), followed by PIK3CA (10.7%). Genomic changes in the RB1 gene are relatively common in TNBCs and loss of Rb protein expression is seen in more than 40% of cases[29].

One of the most found genetic modifications in TNBC is the amplification of the MYC gene which is identified in more than 60% of samples[30].

Gains in chromosomes 1q, 8q, 17q, 20q, and losses in 5q, 6q, 8p are common in breast cancer. Estrogen receptor (ER)-negative cancers frequently harbor losses in 5q and gains in 6p compared with hormone receptor-positive cancers[31]. Secretory breast carcinoma is the only epithelial tumor of the breast with a t (12;15) balanced translocation that makes an ETV6-NTRK3 gene fusion and encodes a chimeric tyrosine kinase[32]. Like salivary gland ACC, the breast adenoid cystic carcinoma shows the t (6;9) translocation leading to the development of MYB-NFIB gene fusion and immunopositivity for MYB by immunohistochemistry (IHC)[33]. High-resolution copy number alteration (CNA) profile in TNBC showed that the most common gains of the entire chromosome arms included 1q,

8q, 10p and 12p, and losses of 5q, 8p, and 17p, and the most frequent focal gains were narrowed down to 3q and 19q and focal losses were identified most often in 3q and 12q[34]. In TNBC, from the genomic loss-of-heterozygosity (LOH) landscape, the most frequent genes exhibiting LOH associated monoallelic expression (MAE) were found within chromosomes 3p, 5q, 8p, 10p, 14, and 17[35].

Among heritable and reversible epigenetic mechanisms, changes in DNA methylation, histones post-translational modifications, and small noncoding microRNAs (miRNA) have been also described in HBCs[36].

Among genes that have been commonly reported to be methylated in breast cancer there are RASSF1A, ERa, PR, RARb, CCND2, and PITX2. Methylation of the BRCA1 promoter is frequent in triple-negative breast cancers (TNBC) and leads to a tumor phenotype similar to BRCA1-mutated tumors[37]. The phenotype that some sporadic tumors share with familial-BRCA cancer is called BRCAness[38]. This status may be due to the hypermethylation of the promoter region of the BRCA1 gene[39].

There are three loci in human chromosome 9p21 as tumor suppressor genes including, CDKN2A (p16INK4a, and p14ARF), and CDKN2B (p15INK4b)[40]. The CDKN2A locus controls the p16INK4a/CDK4/pRb pathway and p14ARF/p53 pathway[41]. The region of the human chromosome, 9p21 encompassing the CDKN2B/CDKN2A or INK4A/ARF/INK4B gene locus, corresponds to regions of dog chromosome 11, mouse chromosome 4, and rat chromosome 5. These regions have been demonstrated to be frequently mutated in various types of cancer[42]. Relative molecular and cytogenetic mapping of the INKA/ARF locus and closely related genes with their positions on human and canine chromosome 9 and 11, respectively(figure 2)[43].

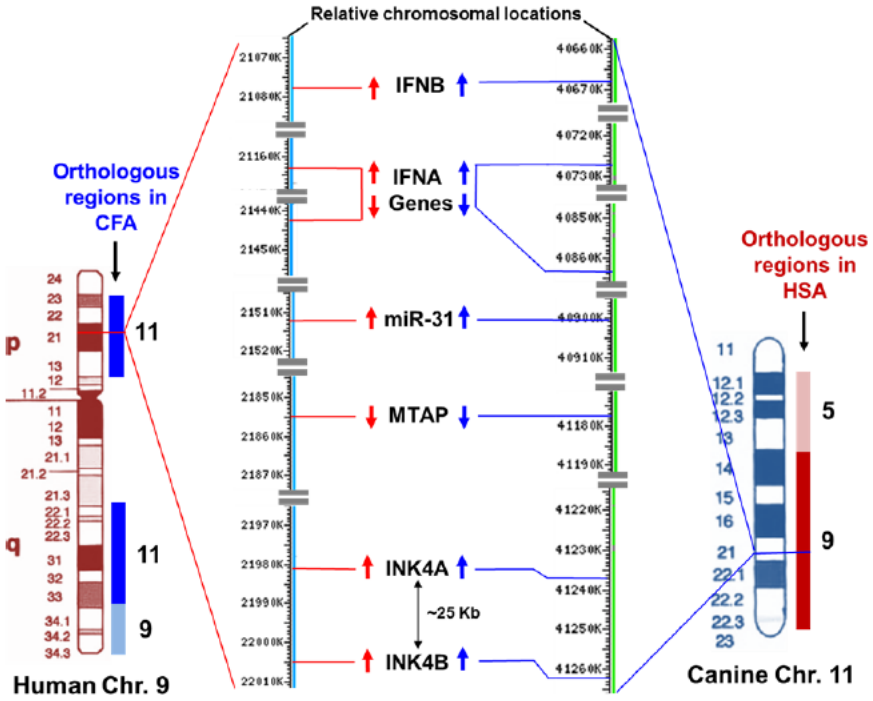

Figure 2- Frequently deleted regions in human chr. 9p21 and orthologous canine chr. 11
Relative molecular and cytogenetic mapping of the INKA/ARF locus and closely related genes with their positions on human and canine chromosome 9 and 11, respectively. The regions at human chromosome 9 and canine chromosome 11 that are frequently deleted in cancers are completely orthologous to each other. The molecular mapping shows the exact chromosomal position of these genes extrapolated from the NCBI map view of each chromosome represented by the current human and canine annotation from releases 106 and 103, respectively. The red and blue arrows indicate the transcriptional orientation of genes in the human and dog chromosomes, respectively. Transcription of genes from the "+ strand" is indicated by down arrows and from the "– strand" by up arrows. (CFA = Canis lupus familiaris; HSA = Homo sapiens; Chr. = Chromosome).

Oncogenic pathways and accompanying genes, such as PI3K/AKT, KRAS, MAPK, Wnt, b-catenin, BRCA2, ESR1, and P-cadherin, are generally up-regulated while tumor suppressive pathways, such as p53, p16/INK4A, PTEN, and Ecadherin, are down regulated in human and canine BC[43].

Loss of the E-cadherin expression is a characteristic of epithelial-mesenchymal transition (EMT). A worse prognosis is associated with low expression of E-cadherin (evaluated by IHC in tumor tissues) in both human and animal patients but it should also be analyzed with other biomarkers, such as Ki67[44].

Several of the human cancer predisposition genes are present in the constitutional (germline) DNA of dogs with cancer; for example, BRCA1/BRCA2 and TP53 germline mutations. In humans, germline mutations of these genes cause hereditary breast and

ovarian cancer syndrome and Li–Fraumeni syndrome, respectively[45]. Liu et al.[13] performed whole-genome sequencing (WES), RNA-seq and/or high-density arrays on 12 CMTs, including seven simple carcinomas and four complex carcinomas and demonstrated that canine simple carcinomas emerge from genomic aberrations while complex carcinomas emerge from epigenomic alterations. Many of the genomic aberrations in canine simple carcinomas accurately reiterate main features of human breast cancer.

CAS comprises various cell types such as fibroblasts, leukocytes, adipocytes, and myoepithelial and endothelial cells and includes extracellular matrix (ECM), soluble factors such as cytokines, hormones, growth factors and enzymes, and physical properties as pH and oxygen content[46]. Amini et al.[47] developed a protocol for laser-capture microdissection (LCM) on formalin-fixed paraffin-embedded (FFPE) tissue sections of 13 canine simple mammary carcinomas to precisely isolate RNA from CAS and normal stroma. After RNA extraction, quality control, quantitation, and preamplification, the relative mRNA levels of selected genes were measured by RTqPCR. Amini et al.[48] confirmed differential expression in CAS compared to the normal stroma of three genes including upregulation of a-smooth muscle actin (a-SMA, encoded by ACTA2), upregulation of collagen 4a1 (COL4A1) and downregulation of vimentin in CAS on protein level utilizing immunofluorescence. Markkanen et al.[49] analyzed CAS and normal stroma from 15 clinical cases using their laser capture microdissection (LCM) coupled with RNA-seq (LCMRNAseq) pipeline to identify stromal reprogramming in canine simple mammary carcinoma on a transcriptome-wide scale. They revealed strong increases in mesenchymal stem cells, gamma delta T-cells, macrophages, plasmoid dendritic cells, and natural killer T-cells in CAS and demonstrated that commonly deranged pathways between canine and human CAS included angiogenesis, epithelial mesenchymal transition, glycolysis, and immune response pathways. To analyze transcriptional reprogramming of adenoma associated stroma (AAS) of 13 canine mammary adenomas compared to previous data from 15 canine mammary carcinomas, Amini et al.[50] applied weighted gene coexpression network analysis (WGCNA) and identified six clusters of highly positively correlated genes and subsequently identified four potentially interesting modules including blue, brown, turquoise and yellow

modules. They showed that TGF-beta signaling, glycolysis, mitotic spindle, epithelial to mesenchymal transition, mTORC1 signaling, unfolded protein response, apical surface, interferon-gamma response and G2M checkpoint demonstrated greatly increased enrichment only in CAS and pathways involving pancreas beta cells, fatty acid metabolism, spermatogenesis, heme metabolism and IL2-STAT5 signaling showing dramatically reduced enrichment only in CAS. Markkanen et al.[49] ranked the samples in The Cancer Genome Atlas (TCGA) breast cancer subset (that contains >1000 human tumor samples) analogous to the stromal enrichment scores to compare their canine-derive stromal signature and found that the canine-derived stromal signature was strongly positively associated with the enrichment of human-derived stromal signature of the TCGA breast cancer subset.

Biomarkers

Biomarkers include genes and genetic variations, differences in messenger RNA (mRNA) and/or protein expression, posttranslational modifications of proteins, and metabolite levels[51]. The principal biomarkers, which are usually immunohistochemically tested on breast surgical specimens, include ER and PR, Mib1/Ki-67, and HER2/neu expression[52].

The estrogen receptor (ER) is a transcription factor that regulates events of gene expression resulting in cell division[53]. Estrogen receptors (ER) include ER-alpha, ER-beta, and a new membrane receptor G protein-coupled receptor 30 (GPR30)[54]. About 75% of breast cancer cases are ERa positive at diagnosis[55]. A member of the nuclear receptor family, the progesterone receptor is a well-known, estrogen receptor (ER)-regulated gene that is expressed in more than two-thirds of ER-positive breast cancers[56]. The human epidermal receptor protein-2 (c-erbB-2; HER2) oncogene protein is a transmembrane glycoprotein in the epidermal growth factor receptor family[57]. IHC is the most used method of assessing these factors, although fluorescent in situ hybridization (FISH) also has a prominent role in HER2 testing[58]. The American Society of Clinical Oncology (ASCO), and the College of American Pathologists (CAP) recommend that ER and PR assays be considered positive if the sample contains at least 1% positive tumor nuclei (fixed in 10% neutral buffered formalin) using the IHC method[59]. ASCO/CAP guidelines, recognize tumors as amplified if the HER2/CEP17 ratio (R) is more than 2.2

or, the absolute HER2 copy number (CN) exceeds 6 in the absence of CEP17 assessments[60]. The TNBC is a subtype of breast cancer that lacks steroid receptors, i.e., estrogen and progesterone receptors, and does not overexpress the HER2 gene[61].

Several pathological biomarkers are used to identify subgroups of TNBC, including Ki-67, epidermal growth factor receptor (EGFR), P53, cytokeratin (CK) 5/6 and CK14[62].

Ki-67 is a nuclear DNA-binding protein expressed in proliferating mammalian cells[63]. It is expressed in cell cycle phase S, G1, G2, and M in the cell nucleus reaching a peak during mitosis. The Ki-67 index is relatively higher in TNBC than in non-TNBC[62].

The human epidermal growth factor receptor (HER) family includes the epidermal growth factor receptor (EGFR), HER2 (erbB2/neu), HER3 (erbB3), and HER4 (erbB4)[64]. It has been reported that at least 50% of TNBC cases have gene amplification or high expression levels of EGFR[65].

Keratins (Cytokeratins) are the intermediate filament (IF)-forming proteins of epithelial cells[66]. 2-D isoelectric focusing and SDS-PAGE were used by Mole et al.[67] to map the keratin profiles of normal human epithelia, tumors, and cultured cells. They grouped keratins into two types, basic to neutral type II keratins as K1-K8 and acidic type I keratins as K9-K19[67]. Genome analyses have recently identified that humans have 54 functional keratin genes, i.e., 28 types I and 26 types II keratins, and form two clusters of 27 genes each on chromosomes 17q21.2 and 12q13.13[66]. Breast ducts are composed of two types of epithelial cells, the inner luminal cells, and the outer basal/ myoepithelial cells. Cytokeratins (CKs) 8 and 18 are expressed in the luminal layer, whereas the basal epithelial layer is characterized by CK5/14 and the transcription factor p63[68]. Basal-like breast cancers typically express basal cytokeratins such as CK5/6, CK14, and CK17. CK5/6 is the most important and relevant marker for defining the basal subgroup of TNBC[69]. c-Kit, a type III receptor tyrosine kinase (RTK), plays a pivotal role in cancer occurrence[70].

Loss of c-KIT expression in breast cancer is related to malignant transformation of breast epithelium and performed by KIT gene promoter DNA hypermethylation[71].

Poly (ADP-ribose) polymerases (PARPs) are a family of related enzymes that share the ability to catalyze the transfer of ADP ribose to target proteins[72]. PARPs constitute a large family of 18 proteins encoded by different genes[73]. PARP1 is the most abundant of

different PARP isoforms and represents more than 90% of PARP's catalytic activity in the cell nucleus[74]. As homologous recombination repair (HRR) pathway is impaired in BRCA1-mutated tumor cells, PARP inhibition in these cells can lead to the accumulation of DNA damage and ultimately induce cell death because of impaired DNA damage repair (DDR) from both base-excision repair (BER) and HRR dysfunctions[75].

The androgen receptor (AR) is a nuclear receptor belonging to the steroid hormone group also including the estrogen receptor (ER), glucocorticoid receptor (GR), progesterone receptor (PR), and mineralocorticoid receptor (MR)[76]. AR seems to play a major role in TNBC carcinogenesis[77]. AR has appeared as a possible therapeutic target for AR-positive triple-negative breast cancer (TNBC)[78].

Programmed cell death protein-1 (PD-1) and programmed death-ligand 1 (PD-L1) are considered as immune checkpoint factors that inhibit the immune reaction to cancer cells[79]. It is assumed that TNBC has a relatively high expression of PD-L1, mainly in inflammatory (immune) cells and sometimes in cancer cells[80].

The signaling pathway of vascular Endothelial Growth Factor (VEGF) is considered important in the pathophysiology of TNBC. Intratumor and serum levels of VEGF are significantly higher in TNBC compared to non-TNBC[81].

The E-cadherin protein (encoded by the CDH1 gene) is normally expressed in breast epithelial tissue and acts as a crucial component of epithelial cell adhesion and epithelial-to-mesenchymal transition (EMT)[82]. Loss of membranous expression of E-cadherin is the defining immunohistochemical feature of lobular differentiation in breast carcinoma[83]. Kashiwagi et al.[84] analyzed the 123 TNBC cases, founding that the prognosis of patients with E-cadherin-negative expression was markedly worse than that of E-cadherin-positive patients.

The Myc oncoproteins (c-Myc, N-Myc, and L-Myc) belong to a family of commonly named "super-transcription factors" that could control the transcription of at least 15% of the entire genome[85]. c-Myc overexpression and Myc dependent gene signatures are features of TNBC[86]. In breast cancer, carcinoembryonic antigen (CEA) and cancer antigen 15–3 (CA15-3) have been the two most widely used serum tumor markers in the clinical fields for more than 30 years[87].

The MUC1 gene is overexpressed in human malignant breast tumors, allowing the use of gene product CA 15-3 as a tumor marker for breast cancer[44]. CA15-3 is a monoclonal antibody-defined tumor marker[88] and carcinoembryonic antigen (CEA) is an oncofetal glycoprotein, a widely used tumor marker due to its high expression in adenocarcinoma[89]. CEA levels are upregulated in TNBC patients and the post- Neoadjuvant Chemoradiotherapy (NCRT) CEA plasma levels may be a potential prognostic factor for Disease-Free Survival (DFS), locoregional recurrence-free survival (LRFS) and distant metastasis-free survival (DMFS) in TNBC patients after received NCRT[90].

The most studied and reliable biomarkers of CMT are Ki-67, EGFR, HER-2, ER, PR, and COX-2, detected in both serum and tissue samples using different molecular methods. Ki-67 expression is the strongest in CMTs with poor clinical and histopathological characteristics[44]. Manuali et al.[91] studied the immunohistochemical expression of CA 15–3 in 7 canine mammary cancer cell lines and 50 malignant mammary tumors and found that CA 15–3 is expressed in both canine mammary tumor cell lines and tissues and that serum levels are significantly correlated with the histological grade. In canine mammary carcinomas, loss of HER2 expression has been associated with a poor prognosis in combination with ER-negative status and positivity of basal cell markers (P-cadherin, p63, cytokeratin 5)[92].

Cell Cycle

Each species on the planet has a set number of chromosomes, arranged in pairs, but each species has a different number of pairs. Humans have 46 chromosomes (23 pairs), dogs have 78 chromosomes (39 pairs), cats have 38 chromosomes (19 pairs), etc. Domestic dogs have the same number of chromosomes as wolves, coyotes, dingoes and jackals(figure 3)[93].

Figure 3- Chromosomes of the domestic dog organized into 38 pairs, according to their banding pattern[93].

The typical cell cycle in eukaryotes is composed of four phases including the G1(gap 1), S (DNA synthesis), G2(gap 2), and M(mitotic) phases. G1, S, and G2 together are called interphase[94](figure 4). During their life span, cells have two possible states: a non-cycling, quiescent state (G0) and a cycling, activated state. Cells may enter a reversible G0 state of quiescence or, alternatively, they may undergo an irreversible G0 state. The latter may be a physiological differentiation or, following a stress event, a senescent status[95].

Both activators and inhibitors regulate the cell cycle, and the function of these regulators is crucial for normal cell growth[96]. Cell cycle progression is mediated by cyclin-dependent kinases (Cdks) and their regulatory cyclin subunits. Cdks, such as Cdk4/6, Cdk2, and Cdk1 (also known as Cdc2) are serine/threonine kinases with a wide variety of substrates. Cdks are activated mainly by binding to their cyclin partners, whose expressions rise and fall throughout the cell cycle to mediate the temporal activation of each Cdks. Various cell cycle checkpoints exist to ensure that critical processes are engaged prior to progression to the next phase. There are three major cell cycle checkpoints, including the G1/S checkpoint (also referred as restriction point), the G2/M DNA damage checkpoint, and the spindle assembly checkpoint (SAC)[97]. CDKs generally lack any protein kinase activity as monomers; formation of a cyclin-CDK heterodimer causes a major refolding of the CDK to a kinase-active form. The cyclin-CDK interface is large, and binding is essentially irreversible. In addition to activation of CDK enzymatic activity, cyclins frequently also contribute ‘docking sites’ that can bind to substrates, thus providing much of the substrate specificity for the heterodimer. The dependence of CDKs on cyclins for enzymatic activity and frequently for substrate

targeting means that CDK activity can be readily controlled indirectly, by control of cyclin abundance, and both transcriptional and post-transcriptional control of cyclin levels are major cell cycle control mechanisms[98]. Cyclin-dependent kinases (CDKs) form a family of 20 serine/threonine protein kinases that exert pivotal functions in fundamental cellular and molecular processes, such as cell division, migration, senescence, death, gene transcription, mRNA splicing, metabolism, and other important mechanisms[99]. As indicated by their name and in addition to post-translational modifications, they require a physical association with a cyclin partner to become catalytically active and able to phosphorylate their protein substrates. Over 30 cyclins have been identified in humans, based on the presence of a cyclin box domain that is responsible for binding and activating CDKs. Functional and phylogenetic studies distinguish 3 subfamilies of CDK and cyclin proteins (cell cycle, transcriptional, atypical) that form combinatorial interactions mostly within each subfamily[100].

Presence of DNA damage activates checkpoints, halting progression of the cell cycle. Arrest for repair, apoptosis or senescence can be triggered both at G1/S and G2/M checkpoints. In the case of senescence-induced DNA damage, it was suggested that G1/S checkpoint is more sensitive and that a single double-strand break (DSB) can induce arrest, while a larger number is required to activate G2/M checkpoint[101]. Overexpression and/or dysfunction of CDKs or cyclins have been reported in a very large number of human cancers and other diverse pathologies. These protein kinases are thus considered as valuable therapeutic targets for drug development. A first set of CDK selective inhibitors have been approved recently against hormone dependent/HER2-negative breast cancers, and they hold promises against other solid tumors[102].

CDKIs are commonly divided in two families:

• One comprises three proteins called p21 (CDKN1A), p27 (CDKN1B), and p57 (CDKN1C) that broadly inhibits multiple CDKs.

• The other family of CDKIs includes p15 (CDKN2B), p16 (CDKN2A), p18 (CDKN2C), and p19 (CDKN2D) that have selective effects on cyclin CDK4 and cyclin CDK6.

Defective CDKI checkpoint proteins allow cells with damaged DNA to divide, resulting in mutated daughter cells at risk for malignant transformation(figure 5)[103].

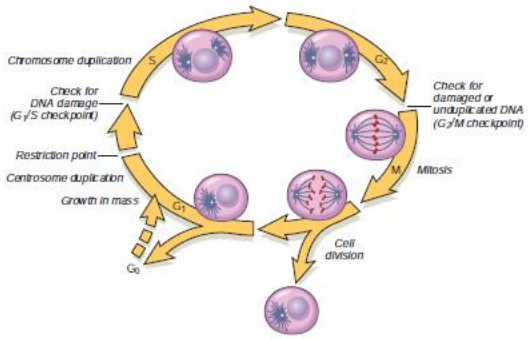

Figure 4- Cell cycle landmarks. The figure shows the cell cycle phases (G0, G1, G2, S, and M), the location of the G1 restriction point, and the G1/S and G2/M cell cycle checkpoints. *G*1 *restriction point* refers to the stage in G1 where the cell is committed to advance further into the cell cycle without requiring any more of the growth signal that initiated cell division. Cells from labile tissues such as the epidermis and the gastrointestinal tract may cycle continuously; stable cells such as hepatocytes are quiescent but can enter the cell cycle; permanent cells such as neurons and cardiac myocytes have lost the capacity to proliferate[103].

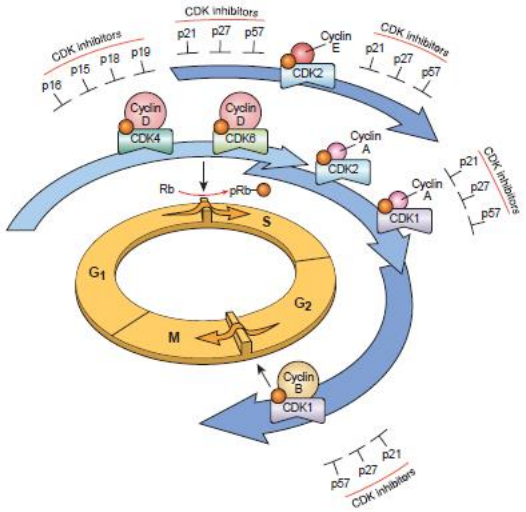

Figure 5- Role of cyclins, cyclin-dependent kinases (CDKs) and CDK inhibitors (CDKIs) in regulating the cell cycle. Shaded arrows represent the phases of the cell cycle during which specific cyclin-CDK complexes are active. As illustrated, cyclin D-CDK4, cyclin D-CDK6, and cyclin E-CDK2 regulat the G1-to-S transition by phosphorylating the Rb protein (pRb). Cyclin A-CDK2 and cyclin A-CDK1 are active in the S phase. Cyclin B-CDK1 is essential for the G2-to-M transition. Two families of CDK inhibitors can block activity of CDKs and progression through the cell cycle. The so-called INK4 inhibitors, composed of p15, p16, p18, and p19, act on cyclin D-CDK4 and cyclin D-CDK6. The other family of three inhibitors, p21, p27, and p57, can inhibit all CDKs[103].

Cell cycle progression is highly regulated by modulating the phosphorylation status of retinoblastoma (RB) family proteins. This process is controlled by a balance in the action of kinases, such as the complexes formed by cyclin-dependent kinases (CDKs) and cyclins, and phosphatases, mainly the protein phosphatase 1 (PP1). The PP1-Spinophilin (SPN) holoenzyme has been described as the main phosphatase responsible for the

dephosphorylation of RB proteins during the G0/G1 transition and at the end of G1[104](figures 6 and 7 [105]).

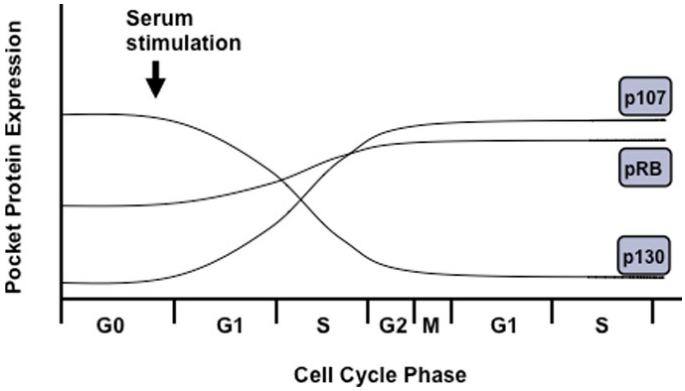

Figure 6- Expression levels of pocket proteins throughout the cell cycle. In G0, the most abundant pocket protein is p130. After cells are stimulated to enter the cell cycle expression of pRB and p107 are induced because they are E2F target genes themselves. At the same time these pocket proteins increase, the expression level of p130 begins to decline. In subsequent cell cycles pRB and p107 remain expressed at relatively constant levels, conversely, p130 is relatively inabundant under these growth conditions. These unique expression patterns offer clear, distinguishing characteristics of each pocket protein family member.

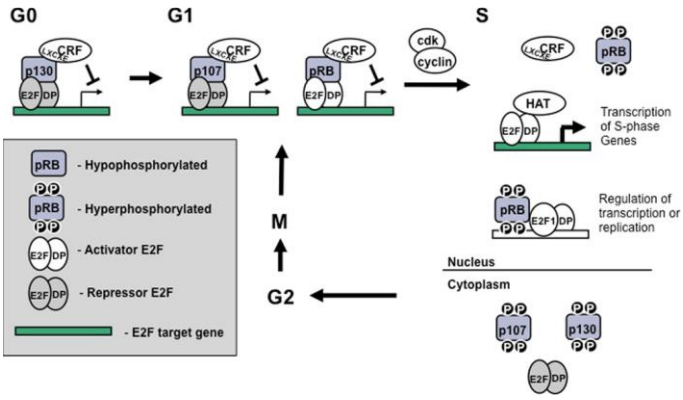

Figure 7- Model of cell cycle entry control by pocket protein. Beginning in the top left corner, quiescent cells repress transcription of E2F targets genes largely through the actions of p130. As cells progress into G1, complexes containing p107 and a repressor E2F such as E2F4 begin to replace p130. Furthermore, complexes of pRB and activator E2Fs such as E2F3 also become more abundant. Chromatin remodeling factors (CRF) are recruited to these complexes and mediate alterations to the chromatin environment, preventing transcription of E2F responsive genes. As a result, transcription of E2F target genes remains low until entry into S-phase. At the transition to S-phase, cyclin/CDK complexes phosphorylate the pocket proteins, dissociating them from the E2F/DP duplexes and transcription of E2F target genes proceeds through S phase. As part of this transition, the repressive heterochromatin changes that were present in G1 are reversed by the recruitment of new enzymes by the E2Fs, histone acetyltransferases (HAT) are examples of this type of enzyme. Another important change at the start of S-phase is the export of p130 and 107 proteins from the nucleus. At this point pocket proteins are thought to be relatively functionless until they are dephosphorylated and reactivated at the end of mitosis so that they can regulate transcription again during the next G1 phase.

Deregulation of cell cycle, via cyclin D/CDK/pRb pathway, is frequently observed in breast cancer lending support to the development of drugs targeting the cell cycle control machinery, like the inhibitors of the cyclin-dependent kinases (CDK) 4 and 6[106]. Inhibition of CDK4/6 can result in different cell fates such as quiescence, senescence, or apoptosis. Senescence is a stress response that can be induced by stimuli that include oncogenic activation, chemotherapy, irradiation, and targeted therapies such as CDK4/6 inhibitors. Senescent cells undergo a stable cell cycle arrest and produce a bioactive secretome that remodels their microenvironment and engages the immune system[107].

Retinoblastoma family of proteins

The retinoblastoma tumor suppressor (RB) protein is functionally inactivated in many human cancers and is aberrant in one-third of all breast cancers. RB regulates G1/S-phase cell-cycle progression and is a critical mediator of antiproliferative signaling[108]. It is known that pRb can be inactivated by various mechanisms including genetic mutations and phosphorylation[109]. The retinoblastoma tumor suppressor gene (RB1) plays a critical role in coordinating multiple pathways that impact cancer initiation, disease progression, and therapeutic responses. Single copy loss on chromosome 13q encompassing the RB1 locus is prevalent in many cancers, yielding reduced expression of multiple genes in cis, and is inversely related to the CDK4/6- RB integrated signature supporting a cause-effect relationship[110]. Loss of pRB function in human cancer occurs predominately via deletion (one copy if heterozygous or two copies if homozygous) of the RB1 gene, RB1 promoter methylation, or mutations resulting in a nonfunctional protein. Deletion of the RB1 gene occurs in 91%–100% of small cell lung cancer (SCLC), 72.2% of basal-like and 61.5% of luminal B breast cancers, 63% of osteosarcomas, 30% of non–small cell lung cancer (NSCLC), and 17%–33% of castration-resistant prostate cancer[111].

RB is believed to be inactivated because of two different mechanisms in breast cancer. 1. RB gene loss, typically because of homozygous deletion, occurs predominantly in triple negative breast cancer (TNBC). This event is relatively rare in ER/PR or Her2 positive cancers at diagnosis. However, in the metastatic setting following treatment with endocrine therapy there is selection for increased loss of RB. 2. RB can also be inactivated by phosphorylation that is initiated by CDK4/6 containing complexes. In breast cancers, amplification of the positive regulators Cyclin D1 and CDK4/6, or loss of

the negative regulator p16ink4a are all known to occur. RB can be activated with CDK4/6 inhibitors[112].

Beyond pRB itself, alterations within the pRB pathway have also been defined as mechanisms of cancer development and/or malignant progression. CDK4 protein expression is often increased in cancer (20%–54%) and point mutations preventing binding to p16INK4 (encoded by CDKN2A) and subsequent inactivation are observed in 16% of breast cancers. Further, elevated protein expression of cyclin D1 due to amplification of the CCND1 gene (2.5%–39%) and chromosomal rearrangement (16%–90%) have been observed in specific cancers[112].

RB pathway disruption is an important part of the progression of intraductal breast carcinoma (BC) and is therefore relevant to the early stages of invasive BC. This suggests that changes in the RB pathway may be associated with malignant transformation, even in the early stages of BC development[113]. It is well-known that dysregulation of cyclin D-CDK4/6-pRb pathway represents a key mediator of endocrine resistance in hormone receptor (HR) positive BC[106].

The RB or RB1gene is part of a larger gene family that includes RBL1 and RBL2, each of the three encoding structurally related proteins indicated as Rb/p105, RbL1/p107, and Rb2/p130, respectively[114]. RB1 gene composition contains 27 exons and 26 introns. Human RB1 gene (GenBank accession number: NM_000321) is in the long arm of chromosome 13 (13q14.2), DNA length of 178 143 bp, mRNA length of 4 772 bp, encoding 928 amino acids[115]. The dog RB1 gene is in the long arm of chromosome 22 (CFA 22q11.2)[116](figure 8[117]).

Chromosome 22 - NC_051826.1

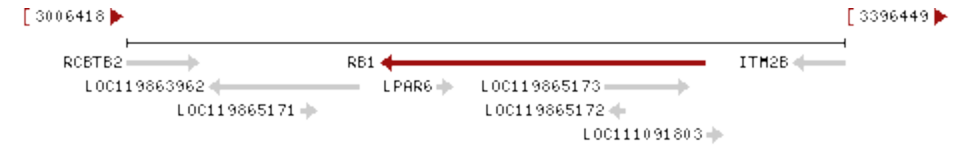

Chromosome 24 - NC_051828.1

Chromosome 2 - NC_051806.1

Figure 8- Canis familiaris RB1, RBL1 and RBL2 genes on chromosomes 22, 24 and 2.

The gene encoding protein pRb is a nuclear phosphoprotein in the molecular mass of about 104-110 kDa[118]. p107 was cloned in 1991 by Ewen et al.[119] and maps on chromosome 20q11.2. The RB2/p130 gene consists of 22 exons, spanning over 50 kb of genomic DNA, and maps to human chromosome 16q12.2, an area in which deletions or loss of heterozygosity has been found in several human neoplasms including breast, hepatic, prostatic, and ovarian cancer[120]. The localization of these proteins into the nucleus or around the nuclear membrane has been shown at the molecular level during the different phases of the cell cycle[121]. Together, these proteins are often referred to as the 'pocket proteins' because their main sequence similarity resides in a domain, the pocket domain, which mediates interactions with viral oncoproteins as well as cellular proteins to exert the biological functions of this family. A spacer region that is not conserved separates the pocket domain into the A and B pockets. The spacers of p107 and p130 but not Rb contain binding sites for cyclin/cdk[122]. All three RB family members contain a conserved domain referred to as the 'pocket' that interacts with the LXCXE motif found in viral proteins such as Tag[123](figure 9[105]).

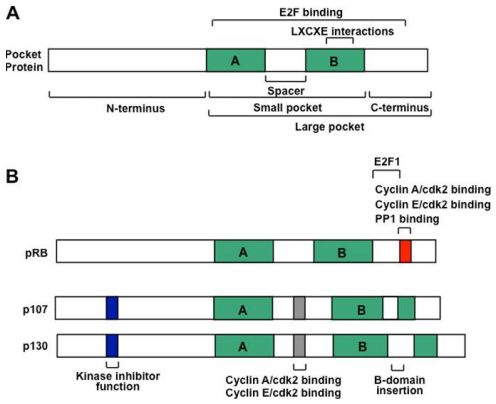

Figure 9- Schematic representation of pRB, p107 and p130 open reading frames. (A) The central feature of RB-family proteins is the pocket domain. It was originally defined as the minimal domain necessary to bind to viral oncoproteins such as simian virus TAg through their LXCXE motif and is denoted as the 'small pocket' in this diagram. The 'large pocket' is the minimal growth suppressing domain of RB-family proteins and it is capable of binding E2F transcription factors as well as viral proteins. (B) Comparison of open reading frame structures of each of the pocket proteins. Note the additional features found in the p107 and p130 proteins, the kinase inhibitory site, the cyclin binding site, and the insertion in the B-domain of the pocket. These provide the most obvious differences between pRB and its relatives p107 and p130.

These structural and biochemical similarities probably explain the functional overlap among pocket proteins during development, and provide rationale for the observation that p107 and p130 can at least partially compensate for loss of Rb function in vivo[124]. RB is widely distributed in various tissues and interacts with many transcription factors and chromatin-remodeling proteins, allowing itself to bind to transcription factors and to modify chromatin structure. In addition to regulating the cell cycle, RB has also been shown to inhibit apoptosis. Consistent with an important role of RB in tumorigenesis, loss of function of RB has been associated with the development of many human cancers[115]. RB proteins exert their effects through binding to E2F transcription factors, which are essential developmental and physiological regulators of tissue and organ homeostasis[125]. The retinoblastoma (RB) protein family members (pRB, p107 and p130) most important target is the E2F-family of transcription factors, which control the expression of genes that mediate G1-S transition. A total of 8 genes have been found, and 10 protein products encoded by these genes form a core transcription axis crucial for regulating cell cycle progression, apoptosis, differentiation, DNA damage repair, metabolism, and angiogenesis. According to initial reporter gene detection and evaluation of their expression patterns during the cell cycle, E2Fs have been classified as

transcriptional activators (E2F1-3) or transcriptional repressors (E2F4-8) The retinoblastoma[126]. During the cell progression through the S into the G2/M phases of the division cycle, pRB undergoes phosphorylation, while in the late M phase, pRB is rapidly dephosphorylated. When pRB is in the unphosphorylated form, it acts as a growth suppressor by repressing transcription of E2F. By contrast, the phosphorylated pRB status (p-pRB) leads to the activation of E2F-responsive genes and entry into the S phase. While Rb/p105 is ubiquitously confined to the nuclei of cycling and quiescent cells, Rb2/p130 activity is also regulated by intracellular localization[127]. RB family of proteins are found in organisms as distantly related as humans, plants, and insects. These proteins play a key role in regulating advancement of the cell division cycle from the G1 to S-phases. This is achieved through negative regulation of two important positive regulators of cell cycle entry, E2F transcription factors and cyclin dependent kinases[128]. The most extensive sequence homology lies in the well-conserved, small pocket region, which consists of A and B domains that are separated by a flexible spacer region[129]. The small pocket is the minimal fragment of pRB that can interact with viral oncoproteins, such as E1A and TAg[130]. Crystallographic data has revealed that the LXCXE motif contacts a shallow groove on pRB, that is among the most well conserved features among pocket protein family members, and among pocket proteins across species[129]. In addition to the viral proteins, a few cellular proteins are reported to contain an LXCXE-like motif that allows them to interact with pRB, p107 and p130[123]. While the overall structure of the pocket domain is well conserved between the three proteins, p107 and p130 are more closely related to each other by sequence similarity than either is to pRB[131]. Two unique features of pRB that have emerged recently are a docking site used only by the E2F1 transcription factor, and a short peptide region in the C-terminus that is competitively occupied by cyclin/cyclin dependent kinases (CDKs) or protein phosphatase 1 (PP1). There are a few of well-known features in p107 and p130 that aren't present in pRB. Both p107 and p130 proteins contain insertions in the B domain of their small pockets. In the case of p130, this insert is subject to regulatory phosphorylation to maintain protein stability[132]. Of the three pocket proteins, p130 has the highest expression level in quiescent cells and at this stage of the cell cycle the majority of E2F complexes contain p130 and E2F4. Recently it has been shown that p130 is part of a transcriptional repressor

complex called DREAM, and it functions to repress E2F target genes during G0[105]. E2F family members 1-3 are referred to as the activator E2Fs because they induce transcription more potently from E2F responsive promoters than other E2F family proteins. E2Fs 4 and 5 are termed the repressor E2Fs because they have limited activation potential. The activator E2Fs associate exclusively with pRB[133]. In early G1, p130-E2F4 is most abundant on the promoters of E2F responsive genes, mediating transcriptional silencing of these genes[105]. In mid- to late G1, when p130 levels drop and p107 levels increase, p107 replaces it at E2F responsive promoters[134]. By late G1, pRB-E2F complexes, whose levels have been increasing throughout cell cycle entry also become more abundant[135]. pRB contains 16 putative Cdk phosphorylation consensus sites spread throughout the protein. In vivo, pRB exists as an unphosphorylated protein in G0 quiescent cells and in two general phosphorylated forms on Cdk sites in cycling cells: hypophosphorylated and hyperphosphorylated[136]. Hypophosphorylated pRB is present in early G1 and contains ;1 to 2 mol of PO4 per mol of pRB[137]. Endogenous D-type cyclins, acting with cdk4/6, can phosphorylate pRb only partially, a process that is likely to be completed by cyclin E-cdk2 complexes. Furthermore, cyclin E-cdk2 is unable to phosphorylate pRb in the absence of prior phosphorylation by cyclin D-cdk4/6 complexes[138]. Analysis of CDK phosphorylation of p107 and p130 is much less extensive than for pRB. However, databases of phosphoproteomic data such as PhosphositePlus suggest that p107 and p130 are also phosphorylated in similar regions surrounding the pocket domain[105]. When cells experience DNA damage during S-phase they need to arrest replication and repair the damage before proceeding. This S-phase checkpoint function has been shown to be absent in RB1 deficient cells, defining a role for pRB in this process. Following DNA damage in S-phase, pRB is dephosphorylated and this allows it to mediate the repression of cyclin A transcription[139]. Generally, hyperphosphorylation, point mutations or protein delocalization lead pocket proteins not to bind their respective E2F partners thereby promoting unscheduled cell cycle progression. However, it is likely that also other molecular mechanisms, which have been previously overlooked, can affect Rb family function in cancer, such as for example post-transcriptional regulation by microRNAs[140]. As well as being phosphorylated, pRB is acetylated, methylated, ubiquitylated, and SUMOylated. Acetylation, methylation, and

SUMOylation play roles in pRB mediated gene silencing. Ubiquitinylation of pRB promotes its degradation and may be used to regulate apoptosis[141]. Markham et al.[142] report that the acetylation of pRb K873/874 occurs in response to DNA damage and that acetylation regulates the interaction between the C-terminal E2F-1-specific domain of pRb and E2F-1. These results define a new role for pRb acetylation in the DNA damage signaling pathway and suggest that the interaction between pRb and E2F-1 is controlled by DNA damage-dependent acetylation of pRb. Beyond these E2F dependent effects on mitosis, non-E2F dependent roles in controlling chromosome architecture are also performed by RB family proteins. Deficiency for all three pocket proteins results in mitotic errors caused by faulty chromatin structure in pericentromeric regions[143]. Importantly, PP1-pRB complexes are most abundant in mitosis, suggesting that this mechanism is part of pRB activation at mitotic exit[144]. In contrast, only protein phosphatase 2 has been shown to dephosphorylate p107 and p130[145]. By mediating histone deacetylation, as well as methylation, pRB contributes to the formation of heterochromatin[146]. Taken together, this suggests that pRB may facilitate a reversible arrest by deacetylating histones and directing a more permanent arrest through histone methyltransferases and gene silencing. Indeed, key cell cycle E2F target genes are reported to be silenced by pRB and a side-by-side comparison revealed that p107 and p130 are dispensable for regulation of these same genes[147]. The ability to recruit chromatin remodeling enzymes to the promoters of E2F target genes is not limited to pRB alone, as both p107 and p130 can repress E2F activity through recruitment of histone deacetylases. However, there is less evidence for p107 or p130 recruiting histone methyltransferases, consistent with pRB having a unique role in gene silencing[105]. Evidence for RB1 mediated tumor suppression is more readily detected across a wider spectrum of tissues and biological contexts while evidence for RBL1 and RBL2 tumor suppressor activity is more restricted. In many cases the tumor suppressor activity of RBL1 or RBL2 is only revealed in the absence of RB1[148]. In addition to regulating the cell cycle, there is growing evidence suggesting that RB proteins might modulate other processes whose dysregulation is associated with tumorigenesis, such as chromosomal stability, cell senescence, apoptosis, and cell differentiation. Thus, it is pivotal to better understand how RB protein levels/activities are modulated and the role that oncogenic

pathways play in this process[149]. In cancer, the RB1 gene is most frequently inactivated through alterations to cyclin dependent kinase regulation, however, in specific cancer types such as small cell lung cancer and retinoblastoma it is uniformly abrogated by direct mutation[128]. The Retinoblastoma protein (RB) and DREAM complex (DP, RB-like, E2F4 and MuvB) cooperate to repress all cell cycle genes during G1 and inhibit entry into the cell cycle. DNA damage activates p53 leading to increased levels of p21 and inhibition of cell cycle progression[150]. In both quiescent and p53 activation conditions, RB and p130 can cooperate to repress G1/S genes, a process that RB plays a predominant role. In the absence of RB and p130, p107 can also repress G1/S genes. Under the condition of DNA damage, p130 and p107 can cooperate to repress the G2/M genes and thus block cell cycle entry into mitosis. In general, when DNA damage leads to p53 activation, RB, p130 and p107 cooperatively repress G1/S genes while p130 and p107 cooperatively repress G2/M genes[115].

Cyclin Dependent Kinases (CDK) inhibitors

CDKs are involved not only in the cell cycle but also in the other critical cellular processes, such as gene transcription, insulin secretion, glycogen synthesis and neuronal functions[151]. So far, 21 CDKs and 5 CDK-like genes have been identified in the human genome based on their homologous sequences[152]. CDK1 emerges as a key determinant of mitotic progression, whereas CDK2 is more associated with DNA replication in higher eukaryotes[153]. In metazoans, cell cycle entry is mostly elicited by CDK4 and CDK6, which are responsive to numerous growth-regulatory signals[153]. Besides cell cycle controlling, some other CDKs including CDK7, CDK8, CDK9 and CDK11, have been shown to participate in transcriptional regulation[151]. CDK7 can phosphorylate RNA polymerase II and contribute to the initiation of transcription[154]. CDK8 is a part of the mediator complex which regulates a plethora of genes[155]. CDK9 can phosphorylate RNA polymerase II and thereby promote elongation of transcription[156]. CDK11 mainly acts on the splicing machinery[156]. There is another type of CDKs, called atypical CDKs, which include CDK5, CDK14, CDK15, CDK16, CDK17, and CDK18. CDK5 is involved in postmitotic functions in specialized tissue settings. CDK inhibitors have been studied since the 1990s[151]. First generation of CDKIs (including Flavopiridol and Roscovitine)

were non-specific pan-inhibitors. These agents induce G1 and G2 phase cell cycle arrest, finally leading to apoptosis. Initially, their effect was attributed to the inhibition of the cell cycle CDKs. However, later studies demonstrated that many of the cellular activities of these inhibitors were probably the result of CDK7 or CDK9 inhibition, the CDKs responsible for regulation of RNA transcription in the mitotic phase of cell division, as well as apoptosis-related genes. The first-generation of pan-CDK inhibitors have poor selectivity and high toxicity, leading to inevitable harmful effects on normal cells[157]. Second-generation CDK inhibitors, including Dinaciclib, P276-00, AT7519, TG02, Roniciclib, RGB-286638 and so on, have been developed with better selectivity and less side effects. Most of the second generation CDK inhibitors have presented efficient anti-tumor activity in preclinical trials, although the safety and efficacy of these inhibitors need to be further verified in clinical studies[151]. More recently, inhibitors specific for CDK4 and CDK6 have entered clinical trials. Such selective inhibitors spare CDK2 activity, avoiding inhibition of general S-phase activity. CDK4/6 inhibitors act downstream of many mitogenic signaling pathways[158]. RB-positive tumor cells respond to CDK4/6 inhibitors(figure 10)[112].

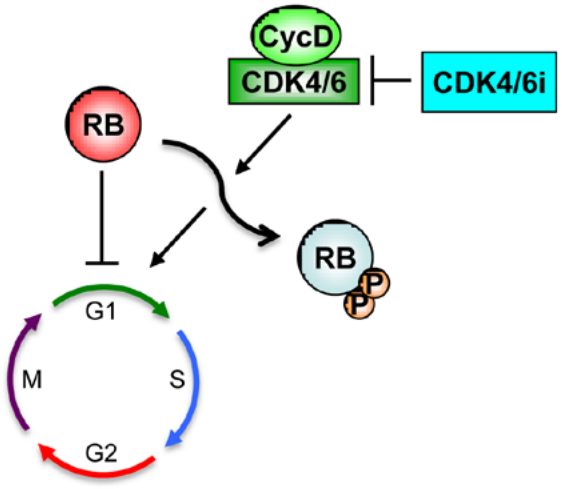

Figure 10- RB positive tumor cells respond to CDK4/6 inhibitors.

Three selective CDK4/6 inhibitors are in late-stage clinical development: ribociclib (LEE011, Novartis), palbociclib (Ibrance®; PD-0332991; Pfizer), and abemaciclib (LY-2835219; Eli Lilly)[159] . Palbociclib has similar potency against cyclin D1/CDK4 and cyclin D2/CDK6. Abemaciclib and ribociclib were noted to have greater potency against

CDK4 than CDK 6. Abemaciclib is 14 times more potent against CDK4 than it is against CDK6. Abemaciclib has five-fold more potency for CDK4 than palbociclib or ribociclib. Unlike palbociclib and ribociclib, abemaciclib has been shown to have in-vivo inhibition of CDK1, CDK2, CDK5, CDK9, CDK14, CDKs16-18, GSK3a/b, CAMKIIg/d and PIM1 kinases. Abemaciclib is 10- to 100-fold less potent against CDK2 and CDK1 than CDK4/6[160]. Pack et al.[161] recently reported that CDK4/6 inhibitor treatment mediates two effects that work together to prevent cell cycle progression: (1) the direct inhibition of CDK4/6-mediated phosphorylation of RB, as the addition of drug leads to a decrease in RB phosphorylation within minutes, and (2) destabilization of CDK4- cyclin D-p21 trimers, allowing non-catalytic inhibition of CDK2 by p21. The latter effect was reportedly specific to CDK4 and p21 and not CDK6 and p27[161]. These Cdk4/6 ATP-competitive inhibitors, which were developed to arrest proliferating cells by inhibiting Rb phosphorylation and inactivation, are the first clinically approved drugs targeting the G1/S transition[162]. Pharmacological inhibitors of cyclin-dependent kinases 4 and 6 (CDK4/6) are now an established standard of care for patients with advanced hormone receptor-positive breast cancer. The canonical mechanism underlying CDK4/6 inhibitor activity is the suppression of phosphorylation of the retinoblastoma tumor suppressor protein, which serves to prevent cancer cell proliferation. Recent data suggest that these agents induce other diverse effects within both tumor and stromal compartments, which explain aspects of their clinical activity[163]. Based on the PALOMA-1trail, FDA approved palbociclib, the first CDK 4/6 inhibitor, in combination with letrozole as first-line treatment for patients with ER-positive, HER2-negative advanced breast cancer (ABC) or metastatic breast cancer (MBC)[164]. The enzymatic activity of CDK4/6 is regulated by several mechanisms[165]. First, several mitogenic signaling pathways that are active in breast cancers positively regulate CDK4/6 activity by increasing *CCND1* expression and/or increasing cyclin D1 protein stability. These include signaling through receptor tyrosine kinases (such as EGFR and HER2), the PI3K–AKT–mTOR axis and the ER[166]. Furthermore, cyclin D1 is a direct transcriptional target of ER, and estrogens promote the transit of ER-positive breast cancer cells from G1 to S phase[167]. Conversely, anti-estrogen therapies such as tamoxifen, aromatase inhibitors, and fulvestrant reduce cyclin D1 expression and hence induce G1 cell cycle arrest. Notably, cyclin D1 can also activate

expression of ER target genes in an estrogen-independent manner. Finally, approximately 15% of breast cancers demonstrate amplification of *CCND1* itself, and these tumors tend to have higher levels of cyclin D1 protein as well[166]. Palbociclib shows *in vitro* enzymatic IC50s for CDK4 and CDK6 of approximately 11 and 15 nM respectively[168]. In clinical practice, palbociclib is typically administered at a starting dose of 125 mg daily 3 weeks on, 1 week off, in conjunction with endocrine therapy[169]. While Rb/p105 is ubiquitously confined to the nuclei of cycling and quiescent cells, Rb2/p130 activity is also regulated by intracellular localization. The phosphorylation status of Rb2/p130 itself is important in the regulation of the cell cycle. The hyperphosphorylated form of pRb2/p130 is cytoplasmic and typical of cells progressing into the G1 phase[121]. An important distinction among the pocket proteins, however, is that Rb, but not p107 and p130, has been shown to be a tumor suppressor in humans[124]. Ventura et al.[149] previously demonstrated that RBL2/p130 is a direct target of AKT and it is a key mediator of apoptosis associated with AKT inhibition. They demonstrated that RBL1/p107 levels are instead not directly modulated by AKT and discovered that RBL1/p107 levels are regulated by multiple pathways linked directly or indirectly to Ca2+-dependent signaling. These novel observations suggest a complex regulation of RBL1/p107 expression involving different components of signaling pathways controlled by Ca2+ levels, pointing out a significant difference with the mechanisms modulating the close family member RBL2/p130[149].

Aims

Aims of this study are:

1. To show CDK4/6 expression in CMT cells and tissues and expression of phosphorylated pRb in CMT tissues.
2. To identify if pablociclib (a CDK 4/6 inhibitor) inhibits pRb phosphorylation in CMT cells.
3. To show the effect of pablociclib on the cell cycle, cell viability, colony formation and CMT cells migration in vitro.

Materials and Methods

Reagents

Palbociclib [PD 0332991($C_{24}H_{29}N_7O_2 \cdot C_2H_6O_4S$)] was purchased from Sigma-Aldrich. Stock solutions of 0.05 mol/L were dissolved in DMSO. For the treatments, the cells were incubated for the indicated times in the presence of Palbociclib (dose range: 1 nM to 10 μM) or the vehicle (DMSO 0.1%). The primary antibodies for immunohistochemistry included the polyclonal rabbit anti-CDK4 (1:100, sc-7180, Santa Cruz) and monoclonal rabbit anti-phospho-Ser807/811-pRb antibody (1:400; CS#8516, Cell Signaling Technologies). The primary antibodies for western blotting included rabbit polyclonal anti-CDK6 (1:500, #sc-928), anti-CDK4 (1:1000; #sc-260) antibodies from Santa Cruz Biotechnology (California), mouse monoclonal anti-pRb (1:1000; #9309) or anti-phosphoSer807/811-pRb (1:1.000; s#5524) antibodies from Cell Signaling Technology (Danvers, Massachusetts), rabbit monoclonal anti-ER α antibody (1:100; ab32063) from Abcam (Cambridge, UK). anti-Rb (C-15), anti-p107 (C-18), anti-p130 (C20), were obtained from Santa Cruz Biotechnology Inc. (Santa Cruz, CA) and used per the manufacturers' instructions. Beta actin antibody (AC-15, ThermoFisher) was used as a loading control. Horseradish peroxidase-conjugated secondary antibodies were from Cell Signaling Technology. The primers used in the present study are ESR1 and GAPDH (table 2)

Table 2- RT-PCR primers from Bio-Rad company

Target Gene	Gene ID
ESR1	qRnoCIP0031419
GAPDH	2597

CMT tissue collection and Canine tumor cells

A total of 45 CMT tumor samples with spontaneous breast cancers were provided at a period of two years (2021-2022). The samples were taken from animals undergoing mastectomy surgery at the OVUD (veterinary teaching hospital of university) of the Department of Veterinary Medicine and Animal Production, University of Naples Federico II and at private veterinary hospitals. Sample collection was carried out during pathological diagnostic with permission of the dog owner approved by a signed informed

consent. A representative fragment of the tumor, which was more than 3 cm in diameter, was collected and divided into two halves. One half of the tumor was subjected to histological analysis. Tissue samples were fixed in 10% formalin for 12–14 h. The fixed tissues were embedded in paraffin, then sections of 4 μm thicknesses were cut and stained with hematoxylin-eosin (HE) for histological classification of each tumor used in this study. Representative portions of each CMT were fixed in 10% buffered formalin, embedded in paraffin wax, and routinely processed. The 4-μm tissue sections prepared from each tumor paraffin block were stained with HE. Histologic examination showed that 21 tumors were malignant. According to Goldscmidt et al.[10] the malignant histologic subtypes included 7 simple and 4 complex carcinomas, 3 carcinoma and malignant myoepitheliomas, 3 solid carcinomas, 2 comedocarcinomas, 1 adenosquamous carcinoma and 1 anaplastic carcinoma. The other half of the tumor was minced into small pieces and enzymatically dissociated in RPMI 1640 (1:1) media (Invitrogen®, Carlsbad, CA, USA) supplemented with 10% fetal bovine serum (FBS, Invitrogen®), 300 UI/ml collagenase (Sigma-Aldrich®, St. Louis, MO, USA), antibiotic-antimycotic solution 100x (Invitrogen®), and 5% of 200 nM glutamine (Invitrogen®). The suspensions with incompletely dissociated tissue were centrifuged at 2.4 x g for 5 min and washed twice in fresh RPMI 1640 media plus antibiotic-antimycotic solution 100 x (Invitrogen®) to proceed cell culture. During the processing of enzymatically prepared cells, fragments of initial tumor were kept generating cell cultures. We prepared five primary CMT cells out of seven simple carcinomas, since preparation of pure primary tumor cells especially from the complex carcinomas, anaplastic and adenosquamous carcinomas and carcinomas with malignant myoepitheliomas was not easy. Canine tumor cells and respective tissue pieces were re-suspended in primary culture medium consisting of RPMI 1640 with antibiotic-antimycotic solution 100 x, 10 % FBS, 5% 200 mM glutamine (Invitrogen®), and plated in 25 cm^2 culture flasks (BD Falcon™, Franklin Lakes, NJ, USA) at an initial concentration of 1.5 x 104 cells/cm2 (Figure 1A and 1B). These cells were grown for 3 h at 38.5 °C and 5% of CO2 in a humidified incubator. After 3 h, the medium was replaced, and the culture conditions were maintained for 24 h. The medium and the tissue fragments were removed and filtered in a cell strainer 70-μm filter (BD Falcon™). At this point, the new medium consisted of F12/Dulbecco's

Modified Eagle Medium (DMEM) (Invitrogen®), antibiotic-antimycotic 100 x (Invitrogen®), 10% FBS, and 5% 200 mM glutamine (Invitrogen®). Under this condition, culture flasks were kept in a humidified incubator at 38.5 °C and 5 % CO2 until complete monolayer confluence. The medium was refreshed every 24 h, and pictures were taken to observe the morphology at 5-day intervals under an inverted microscope (Olympus IX 70, Tokyo, Japan). The unstained sections were kept for immunohistochemistry analysis of cellular markers.

Cell viability

To explore the sensitivity of CMT cells to palbociclib, we first examined the half-maximal inhibitory concentration (IC50) of pablociclib using the cell counting kit-8 (CCK-8) assay (Dojindo Laboratories, Kumamoto, Japan). with palbociclib (Sigma-Aldrich) at various concentrations (0, 0.01, 0.1, 1, 10, and 100 μM) in 96-well plates for 48 hr. The cell proliferation was assessed by adding 10 μL WST-8 (2- [2-methoxy 4-nitrophenyl]-3-[4-nitrophenyl]-5-[2,4-disulfophenyl]-2H-tetrazolium, monosodium salt) and incubated for 4 hr. Absorbance was measured at a wavelength of 450 nm. The IC50 was calculated from drug survival curves. The IC50 values of palbociclib was analyzed using one-way ANOVA. Statistical significance was set at $P < 0.05$.

Immunohistochemistry

In total, 5 cases of mammary carcinomas from different dog breeds were analyzed for CDK4 and ppRb expression. The paraffin-embedded tumor samples were cut to 4 μm thickness and subjected to IHC assay. The standard avidin-biotin-peroxidase complex (ABC, DakoCytomation®) method was used. Unstained sections were deparaffinized, rehydrated, and washed in buffered saline with 0.1% Tween 80. Antigen retrieval was carried out in the microwave with citrate buffer (pH 6.1) for 15 min at 700W, normally damaged by formaldehyde fixation. Before staining, the slides were treated three times with 50% hydrogen peroxide for 30 min to inactivate the endogenous peroxidase and were then rinsed five times in buffered saline for 10 min each to remove remainders. The subsequent step consisted of blocking nonspecific binding by incubating in 15% reconstituted dry skim milk for 90 min. The slides were overlaid by primary antibodies

overnight at 4 °C in a humidified atmosphere. After washes with buffered saline, 200 µl of the secondary antibody was incubated was added to each slide and incubated for 1 h at 37 ºC, and then, 100 µl streptavidin-peroxidase complex (DakoCytomation®) was added to each slide and incubated for 1 h at 37 ºC. In addition, a substrate made fresh in the dark, by mixing equal volumes of 0.02% hydrogen peroxide and 0.6 mg 3,3-diaminobenzidine tetrahydrochloride (DAB; Sigma-Aldrich®), was added to the slides at room temperature. The reaction was stopped by washing with tap water, and the specific brown color was revealed after counterstaining with Mayer's Haematoxylin. A highly brownish accumulation was taken as control positive, while the absence of the primary antibody was considered as a negative control for the several antibodies. The primary antibodies were the polyclonal rabbit anti-CDK4 (1:100, NBP1-3130, Novus Bio.) and monoclonal rabbit anti-phospho-Ser807/811-pRb antibody (1:400; CS#8516, Cell Signaling Technologies).

RT-qPCR

CMT cells were lysed in TriFast reagent (PeqLab Biotechnology, Erlangen, Germany), and total RNA was extracted using the Directzol RNA Miniprep kit (Zymo Research, Irvine, California) including an incolumn DNase I treatment. RNA concentrations were measured on a NanoDrop 2000c UV spectrophotometer (Thermo Fisher Scientific, Waltham, Massachusetts). To isolate RNA from cells, CMT cells pellets were lysed in RLT buffer (included in the RNeasy mini kit, Qiagen) containing 10% ß-Mercaptoethanol (Merck). RNA was isolated from cells using the RNeasy mini kit (Qiagen, cat. n. 74104) according to the manufacturer's procedure. The optional DNase digestion step was also included. To perform reverse transcription and quantitative real-time PCR, cDNA was synthesized using the RevertAid First Strand cDNA Synthesis Kit (Invitrogen) with random hexameric primers. In the qPCR reactions, an equivalent of 10 ng RNA was used with 3 µl 1.5µM primermix (Biolegio, Nijmegen, the Netherlands), containing both forward and reverse primers, and 12.5 µl SYBRR Green mastermix (Bio-Rad, cat. n. 4364346, California, USA) in a 25 µl reaction. For all primer sets, optimum melting temperatures were determined. Additionally, PCR amplification efficiencies were tested using 10-fold dilution series of cDNA. Using the BioRad CFX Connect real-time PCR detection system (Bio-Rad, cat. n. 1855201), an initial denaturation step was

performed at 95◦C for 3min, followed by 40 cycles of denaturation at 95◦C for 10 s, and annealing/extension at 61◦C for 30 s[170]. All reactions were performed in duplicate and negative controls were included. For RNA derived from the cultured cells the normalized expression was presented relative to the expression level of the same genes in the control (untreated) samples (delta delta Ct method)[171]. Real time quantitative polymerase chain reaction (RT-qPCR) primer and hydrolysis probes for the target gene canine ESR1 and the reference gene GAPDH were designed using the PrimerQuest primer design tool (Integrated DNA Technologies, Skokie, Illinois). The primers for the housekeeping gene and for the target gene are shown in Table 3.

Table 3- Primer sequences

Gene	Primer sequence
GAPDH	Forward: TGTGTCCGTCGTGGATCTGA Reverse: TTGATGTTGAAGTCGCAGGAG
ESR1	Forward: GCCCTATTACCTGGAGAACGA Reverse: TCACTGGTACTGGCCAATCT

Western blotting

CMT cells were cultured in 12-well plates to confluency of approximately 80% and exposed ¼ IC50 to 4xIC50 of pablociclib(Sigma-Aldrich, Germany) for 12 hours, or IC50 Palbociclib for 1 to 12 hours. For ER expression analysis, CMT cells and MCF7 were grown to 100% confluency in a 6-well plate, washed with phosphate-buffered saline (PBS) and lysed with 350-µL RIPA buffer. Treatment was stopped by placing the plate on ice, removing incubation medium and addition of 100-µL lysis buffer (62.5 mM Tris-HCl, 2% w/v SDS, 10% glycerol, 50 mM DTT, 0.01% w/v bromophenol blue, pH 6.8) per well. Whole cell lysates were transferred to an Eppendorf tube and denatured at 95 degrees Centigrade for 5 minutes with palbociclib at indicated doses and for indicated times. Control cells were treated with DMSO alone. After 72 hours of incubation, the cells were harvested on ice, washed with cold PBS and lysed in lysis buffer consisting of 50 mM TRIS-HCl pH 7.5, 50 mM EDTA pH 8, 150 mM NaCl, 1% NP40, 2 mM NaOV, 10 mM NaF, 0.3 mM PMSF, a protease inhibitor cocktail (Roche), and the phosphatase inhibitor cocktail 3 (Sigma-Aldrich). After 30 min at 4 degrees Centigrade, the mixtures were centrifuged at 12000 g for 15 min and the supernatants were analyzed by western

blotting. For western blot analysis, equal amounts (30 ug) of cell lysates were resolved in 10% SDS-PAGE (6-8% for Rb, p107, and p130) and then transferred to nitrocellulose membranes (Bio-Rad). After blocking with 5% nonfat milk in Tris-buffered saline with Tween20 (TBS/T) (150 mM NaCl, 10 mM Tris-HCl, pH 8.0, 0.05% Tween 20) for 1 hour, membranes were incubated at 4 degrees Centigrade overnight with the following antibodies: rabbit polyclonal anti-CDK6 (1:500, #sc-928), anti-CDK4 (1:1000; #sc-260) antibodies from Santa Cruz Biotechnology (California), mouse monoclonal anti-pRb (1:1000; #9309) or anti-phosphoSer807/811-pRb (1:1.000; s#5524) antibodies from Cell Signaling Technology (Danvers, Massachusetts), rabbit monoclonal anti-ER α antibody (1:100; ab32063) from Abcam (Cambridge, UK).). anti-Rb (C-15), anti-p107 (C-18), anti-p130 (C20), were obtained from Santa Cruz Biotechnology Inc. (Santa Cruz, CA) and used per the manufacturers' instructions. Anti-beta Actin antibody (1:2000, AC-15, ThermoFisher AB2536382) served as loading control. Membranes were washed three times with TBS/T and incubated with horseradish peroxidase-conjugated antirabbit or anti-mouse IgG antibody (Cell Signaling Technology) for 1 hour at room temperature (RT). The signals were detected using the Super signal West Pico Chemiluminescent Substrate (Pierce) and imaged with Bio-Rad Chemidoc XRS+ (Bio-Rad) and analyzed with Image Lab software (Bio-Rad).

Fluorescence-activated cell scanning (FACS) analysis

For cell cycle analysis, CMT cells were treated with 0.65 μM Palbociclib for 8, 18 or 48 hours and collected by centrifugation (200g, 5 minutes). After incubation with 100 μg/mL RNase A (30 minutes; 37 degrees Centigrade), cells were stained with 20 μg/mL propidium iodide (PI) for 30 minutes at 37 degrees Centigrade. To assess apoptosis, CMT cells were treated with 0.65 μM Palbociclib for 12, 24 or 48 hours and analyzed for Annexin V expression by using Annexin V-FITC Apoptosis Staining Kit (BD Biosciences, Franklin Lakes, New Jersey). Stained samples were measured by using a BD FACSCanto II flow cytometry system, and analyzed with FlowJo software (version 10, TreeStar Inc., Ashland, Oregon). All experiments were performed in duplicates and repeated three times.

Colony forming assay.

Clonogenic assay or colony formation assay is an in-vitro cell survival assay based on the ability of a single cell to grow into a colony[172]. Clonogenic assay can be used to determine the effectiveness of cytotoxic agents. CMT cells were seeded in 100 mm in diameter petri dishes (Euroclone) with a density of 100 cells/dish and 24 hr after seeding were treated with different concentrations of Palbociclib. After 10 days, during which the medium was refreshed every 2 days, the colonies were fixed with 4% paraformaldehyde for 20 min and stained with crystal violet (Sigma-Aldrich, St. Louis, MO). The cell colonies were photographed under an inverted microscope (Zeiss, Germany).

Cell migration

This simple and popular assay allows observation of two-dimensional (2D) cell migration in confluent, monolayer cell cultures[173]. Wound healing assays were performed to investigate cell migration in response to treatment. CMT cells were grown to confluence in 100 mm tissue culture dishes. Cell layers were scraped with a sterile pipet tip, then the medium was discarded, and cells were rinsed twice by PBS. Subsequently, the cells were treated with palbociclib at sub-toxic concentrations (0.32 and 0.65 uM) or DMSO and incubated at 37 degrees Centigrade. Photographs of the movement of cells into the scratch area were taken every 24 h until the scratch area had closed using a Leica DMIL microscope (Leica Microsystems, North Ryde, NSW, Australia).

Spheroid assay

Spheroids are an in-vitro model of the structural organization of tumor tissue, and oxygen and nutrients availability are known to be very limited at the center of a spheroid[174]. Cancer spheroids are widely used to assess tumor response and sensitivity to chemotherapeutics, combination therapies and drug delivery vehicles[175]. For spheroid inhibition assay, CMT cells (1000/well) were seeded in 96 well plates with low cell attachment surface (Thermo Scientific™ Nunclon Sphera™, Waltham, MA), using a sub-toxic concentration (0.32 um) of pablociclib or an equal amount of DMSO. Spheroids were observed under an inverted microscope and photographed at 3 and 5 days after seeding. Experiments were performed in triplicate.

Statistical analysis

The statistical analysis was performed using Graphpad Prism Software. Statistically significant differences among the means of multiple matched groups were evaluated by one-way repeated measures Anova with Dunnett post-test, to compare all data versus control. To evaluate statistically significant between the means of two matched groups, we used the two-tailed paired Student t-test. $P< 0.05$ was statistically significant.

Results

pRb, pRb107, pRb130 and CDK4/6 expression in CMT cells

We tested the CMT cells for the presence of estrogen receptor at the mRNA and protein levels. RT-PCR analysis showed no ER mRNA in CMT cells (Table 1). Immunoblotting using an anti-human ERα antibody revealed an approximate 66-kD band in human MCF7 cells, which was used as positive control. The ERα antibody failed to detect a protein with a similar size in CMT cells. Therefore, the CMT cells did not express ER (figure 1). Western blotting of CMT cells for the expression of CDK4 (30 kDa) and CDK6 (60 kDa) proteins showed that all the CMT cells expressed both proteins except the CMT 5 cells that did not express CDK6 (figure 2). Furthermore, Western blotting of CMT cells for the presence of pRb, pRb107 and pRb130 showed that all the cells expressed pRb, and all the cells except CMT1 cells expressed pRb107 and pRb130 (figure 3). CMT2 and CMT3 expressed both CDK4, and CDK6, and all the Rb family of proteins. Thus, we chose CMT3 for further investigation.

Table 1: Real-time PCR analysis of expression of canine ER (ESR1) and GAPDH in CMT cells (cq: quantification cycle)

CMT cells	GAPDH house- keeping gene. mean Cq 14.49	ESR1 mean Cq 41

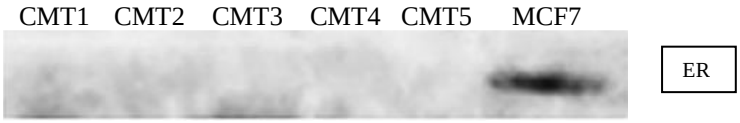

Figure 1- Western blot of ER protein in CMT1 to CMT5 cells and MCF7 cells. CMT cells do not express ER. MCF7 cells express ER and were used as positive control.

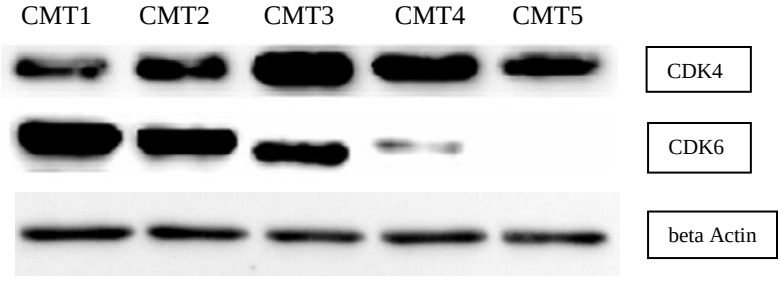

Figure 2- Western blot of CDK4 and CDK6 proteins in CMT1 to 5 cells. All the cells express CDK4 and CDK6 except CMT5 that does not express CDK6.

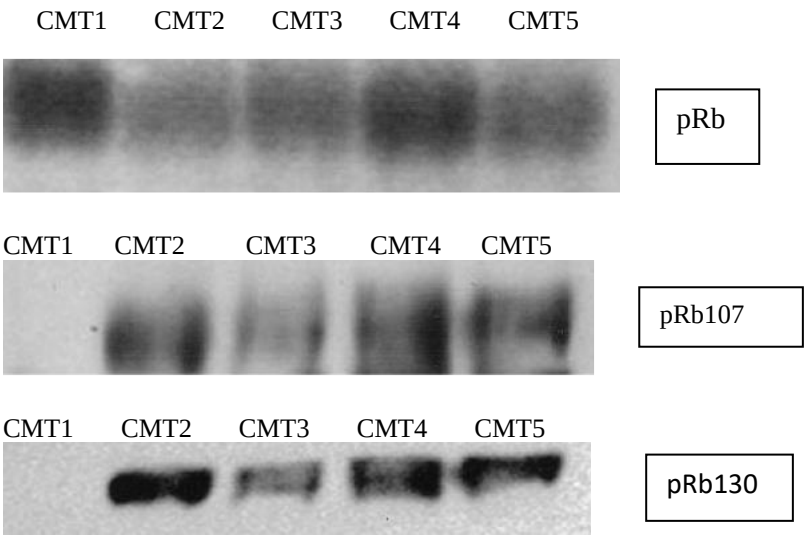

Figure 3- Western blot of pRb, pRb107 and pRb130 proteins in five CMT cells. Rb protein is detectable in all the cells. Rb protein is present in all CMT cells except CMT1.

Expression of CDK4 and pSer807/811 pRb in canine mammary cancer tissues by immunohistochemistry

To obtain insights concerning CDK4 and p-pRb expression in vivo, two canine mammary carcinomas were analyzed by immunohistochemistry. Staining revealed a diffuse expression of CDK4 in the nucleus and/or cytoplasm in both samples. Regarding p-pRb, only one tissue showed a positive staining (figure 4). The staining intensity was evaluated compared to the surrounding stroma.

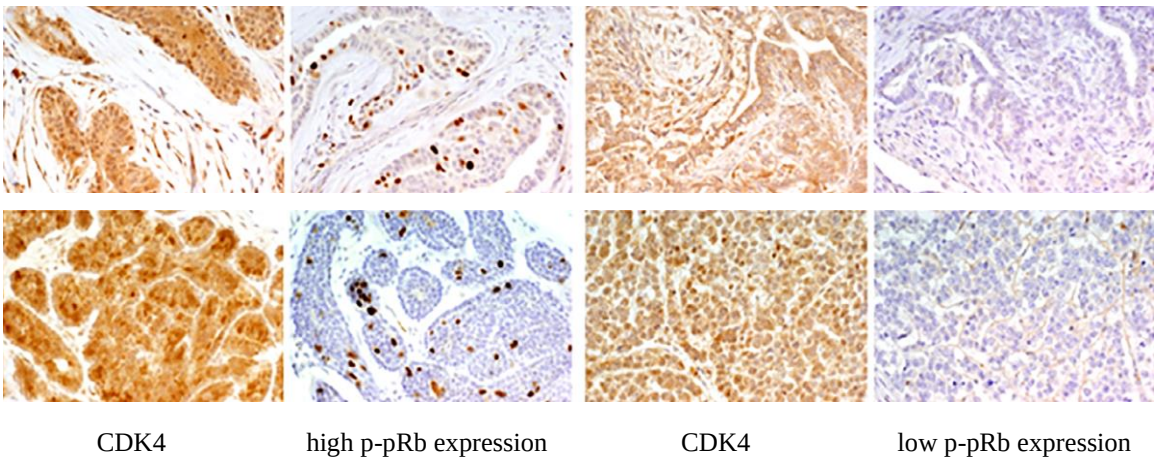

Figure 4- CDK4 and p-Ser807/811 pRb expression in two canine mammary carcinomas. Photomicrographs of canine complex carcinomas with both positive CDK4 and high (right) or low expression of pSer807/810pRb (p-pRb) (left).

Palbociclib inhibits phosphorylation of Rb family of proteins in CMT cells.

In order to assess the the half-maximal inhibitory concentration (IC50) of palbociclib on our cells, we used counting kit-8 (CCK-8) assay (Dojindo Laboratories, Kumamoto, Japan). CMT cells were treated with palbociclib (Sigma-Aldrich) at various concentrations and IC50 was calculated. In Figure 5 is reported the dose response curve of CMT3. The IC50 for these cells was 65.13 nM.

We then determined the effect of Palbociclib on the activity of phosphorylated pRb.

CMT cells were exposed to increasing concentration of palbociclib, ranging from ¼ IC50 to 4xIC50 for 12 hours and then examined for Rb phosphorylated on Ser807/811. Immunoblotting showed the presence of p-pRb in CMT3 cells. Treatment of CMT cells with Palbociclib resulted in a concentration-dependent loss of p-pRb (figure 6). The total amount of pRb, remained largely unaffected. Dephosphorylation of Rb was also assessed after cell exposure to 0.65 μM Palbociclib for 2 to 12 hours. A reduction of p-pRb abundance was observed after 10 hours in CMT3 cells (Figure 7).

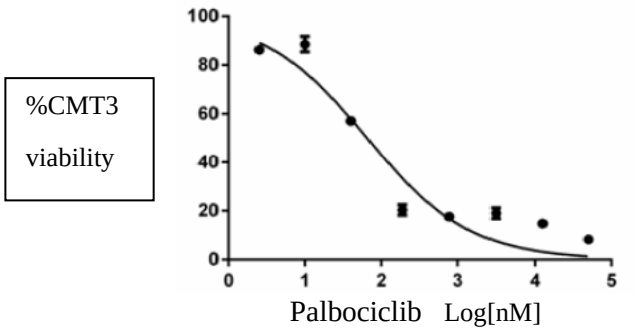

Figure 5- Dose-response curve of CMT3 cells treated with Palbociclib. The cells were treated for 12 hours with indicated concentration of Palbociclib. The results are the mean of three independent experiments.

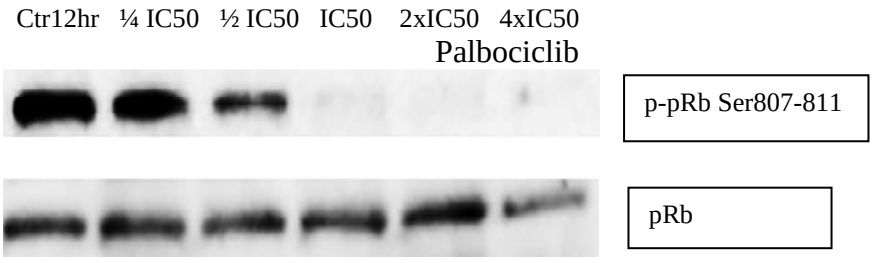

Figure 6- CMT3 cells were incubated with indicated Palbociclib concentrations for 12 hours and analyzed for total pRb (pRb) and Ser807/811-phosphorylated pRb (p-pRb) expression by Western blotting. Palbociclib decreases Rb phosphorylation of CMT cells in a dose dependent manner. (Ctr 12 hr. cells were cell without treatment)

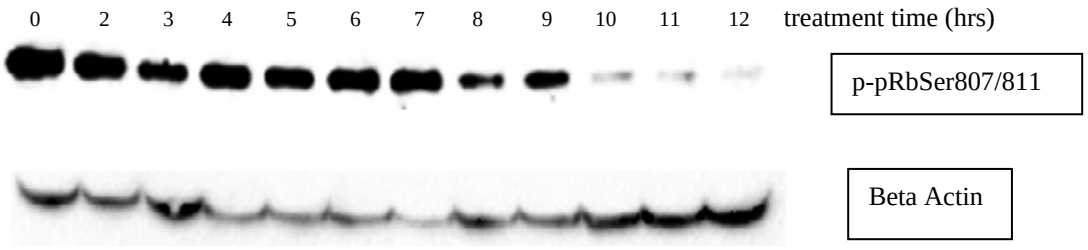

Figure 7- CMT3 cells were exposed to 0.65 μM Palbociclib for 2-12 hours and analyzed for protein expression of pSer807/811-pRb (p-pRb) by immunoblotting. Beta actin was used as loading control. Palbociclib decreases Rb phosphorylation of CMT cells in a time dependent manner.

The expression pattern of Rb family of proteins pRb105, pRb107 and pRb130 were evaluated in CMT3 cells treated with 0.65 um of palbociclib for two hours to eight days compared with serum starved (Q) and asynchronously growing (log) cells. We found that levels of the RB family member p130 increased approximately 1 day after palbociclib (0.65 um) treatment in CMT3 cells compared to log-phase cells and remained elevated for at least 5 to 8 days. p130 was predominantly in its slower-migrating, hyperphosphorylated form in asynchronously growing log-phase cells and in cells treated for 2 or 4 h. Eight hours following drug treatment, p130 appeared as a doublet representing both hyper- and hypo-phosphorylated forms and, 1 day to 8 days later, predominated in the hypophosphorylated form). p107 levels decreased after drug treatment. No changes in p107 phosphorylation status were detected by changes in migration position. RB levels declined although, as with p130, treatment did result in an increase in the faster-migrating hypophosphorylated band (empty arrow), first appearing as a doublet at 8 h compared to the hyperphosphorylated form, which was prominent in log-phase cells and cells treated for 2 or 4 h. (figure 8).

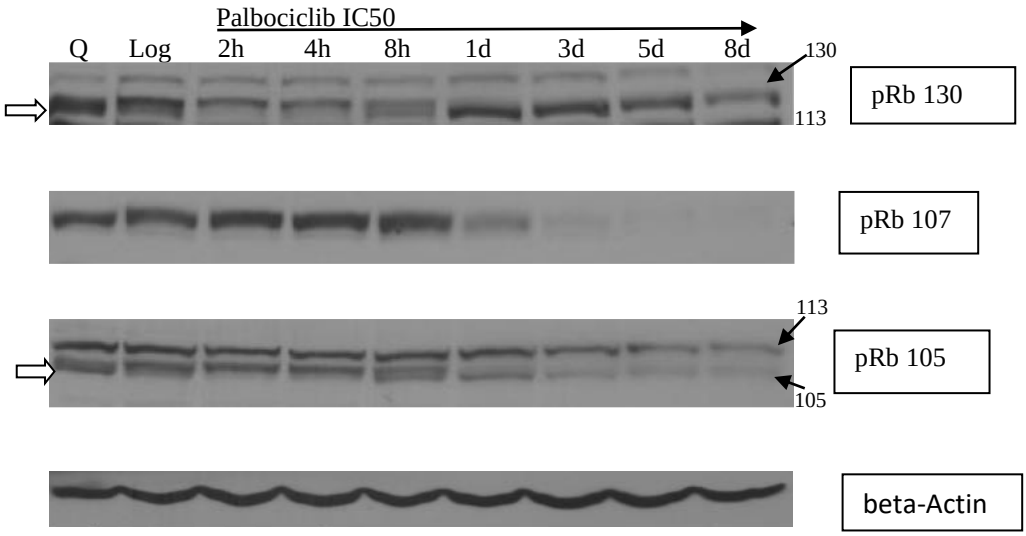

Figure 8- Western blotting shows changes in levels and phosphorylation status of RB family members pRb105, pRb107 and pRb130) in Palbociclib treated CMT3 cells. Subconfluent CMT monolayers, serum starved for 2 days (Q) and asynchronously growing (Log). Beta-Actin was a loading control.

Effects of Palbociclib treatment on the cell cycle and cell viability

To test the effect of Palbociclib on the cell cycle, CMT3 cells were treated with 0.65 μM Palbociclib for 8 hours and analyzed for DNA content by flow cytometry. Compared with non-treated controls, the proportion of CMT cells in G0/G1 phase increased significantly after Palbociclib treatment. The number of cells in S phase and G2/M phase decreased. To assess the effect of Palbociclib treatment on cell viability, CMT cells were treated with 0.65 μM Palbociclib for 12, 24 or 48 hours, and examined for apoptosis by Annexin staining. Exposure to Palbociclib for 48 hours, significantly reduced the amount of vital CMT3 with an increase in the apoptotic cell population. Thus, exposure to Palbociclib for 48 hours seems to affect the viability of CMT cells.

Palbociclib impairs migration of canine breast cancer cells.

We also tested the effects of Palbociclib on cell migration ability. Hence, we performed a scratch test on CMT3 cells and evaluated cells' ability to close the wound upon 24 and 48 hours of treatment with sub-toxic doses of Palbociclib (1/2 IC50 and IC50). We found that both treatments affected cell migration, impairing their ability to migrate and heal the

wound, compared with control cells treated with DMSO. We took the Photographs at indicated time points. We did the experiments in triplicate. The concentrations of palbociclib were not toxic at 48 h. (figure 9).

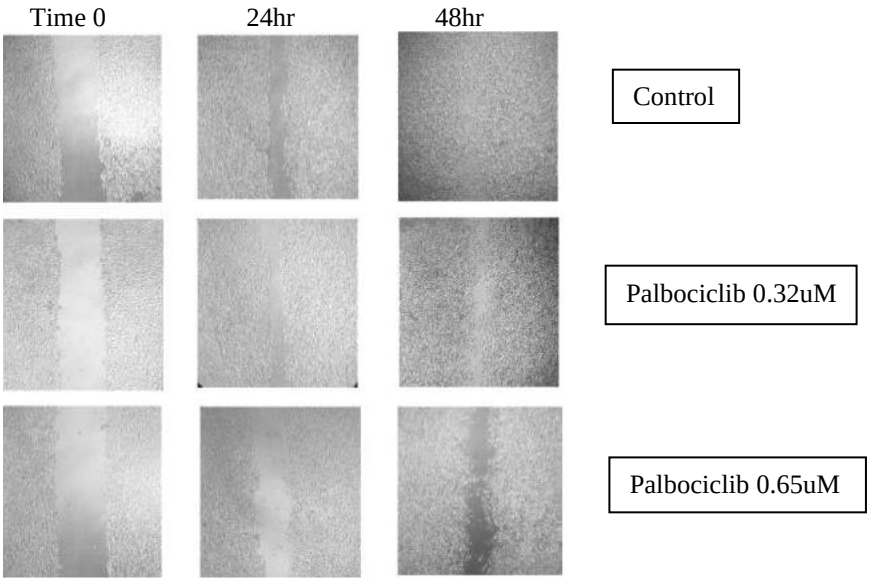

Figure 9- Palbociclib impaired migration ability of CMT3 cells. CMT3 cells migrate into a wound created in a confluent culture plate. Cells migrated into the wound over the 24 and 48 hours, and migration was significantly inhibited in the presence of subtoxic concentrations of Palbociclib.

Palbociclib affects proliferation of CMT spheroids.

CMT3 cells were seeded in ninety-six well low-attachment plates with or without treatment with sub-toxic concentrations of palbociclib. Palbociclib inhibited spheroid formation (figure 10).

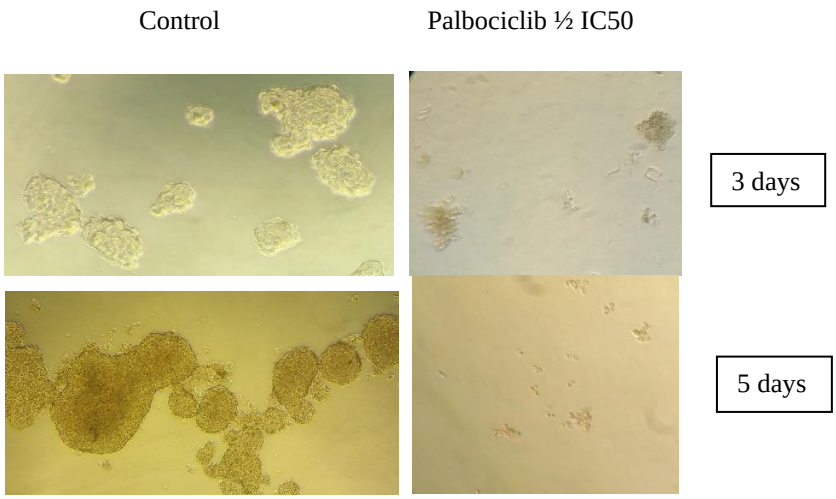

Figure 10- Palbociclib inhibits spheroid formation in CMT cells (1000 cell/well 40x).

Palbociclib inhibits colony formation.

24 hours after seeding, CMT3 cells were treated with different concentrations of palbociclib and allowed to grow for 10 days, during which the medium was refreshed every 2 days. Control cells were treated with an equal amount of vehicle (DMSO). After fixing, the colonies were stained with crystal violet. The cell colonies were photographed and enumerated under an inverted microscope. The colonies decreased in number in a dose-dependent manner (figure 11).

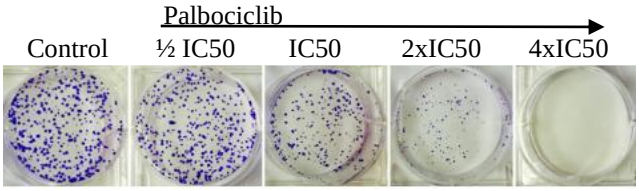

Figure 11 – Palbociclib shows dose-responsive decrease in number of colonies.

Discussion

Primary cells represent the in vivo tissue environment. As these cells are derived directly from native body tissue, they mimic the in vivo state and physiology. When primary cell cultures undergo genetic transformation, they divide indefinitely and become immortalized secondary cell lines[176]. The great advantage of using CMT-derived culture cells is an unlimited source of homogenous self-replicating material. There are general environmental differences between cancer cells growing in vitro and heterogeneous tissue in vivo[177].

Surgery is the primary treatment in the control of CMTs. Additional treatment (adjuvant therapy) can be given after the primary mammary cancer treatment to lower the risk of developing further recurrences and metastasis. Adjuvant therapy may include chemotherapy, radiotherapy, and targeted or individualized therapy, this latest based on the specific genetic characteristics of the cancer in a patient[6]. We tested whether Palbociclib, a CDK4/6 inhibitor approved for treating advanced, ER positive mammary tumors in human patients, may represent a candidate for treating CMTs. Our primary CMT cells had no detectable ER protein and ER mRNA was sparsely found, thus our CMT3 cells were ER negative.

For this study we chose CMT3 cells among the cells that expressed both CDK4, and CDK6, and all the Rb family of proteins. The significance of Rb phosphorylation at different sites is suggested by the observation that Rb function may be modulated according to the location at which it is phosphorylated. Hyperphosphorylation at serine 780, serine 807/711, and threonine 821/826 appears to be involved in the disruption of E2F binding to Rb[178].

Treatment of CMT3 cells with different doses of palbociclib (¼IC50 to 4xIC50) for 12 hours determined a decrease in p-pRb$_{Ser807/811}$ (a preferential CDK4/6 phosphorylation site). Treatment of CMT3 cells with a dose of IC50 for 12 hours showed that p-pRb$_{Ser807/811}$ started to decrease after 10 hours. Therefore, palbociclib activated pRb in dose and time dependent manner.

Moreover, we found that the treatment CMT3 cells with palbociclib with a dose of IC50 for 2 hours to 8 days differently modulates phosphorylation of each Rb family member (pRb105, pRb107 and pRb130). CMT cells. Both pRb105 and pRb130 showed the

appearance of faster migrating hypophosphorylated bands after 8 hours and showed an increase in the intensity of the hypophosphorylated bands in comparison with the hyperphosphorylated bands after day 1. Palbociclib decreased the level of pRb107 with no noticeable change in phosphorylation during the same time. Therefore, both pRb105 and pRb130 and not pRb107 were activated in a time dependent manner with palbociclib treatment in CMT cells.

Cell migration plays an important role in both physiological and pathological processes ranging from embryonic development to angiogenesis and tumor metastasis. The scratch assay or wound healing assay is a commonly used technique to evaluate directed cell migration[179]. Multicellular tumor spheroids are the most widely used 3D in vitro model in preclinical cancer research, reproducing important aspects of tumors, such as the presence of oxygen and nutrients gradients, and subpopulations of quiescent cells[180].

We also demonstrated that subtoxic concentrations of palbociclib inhibited migration of CMT cells and inhibited tumor spheroid formation meaning that it can prevent invasion and metastasis of tumor cells. Palbociclib also inhibited colony formation and showed its cytotoxic effect in a dose responsive manner. Pablociclib increased the population of cells in G1 phase of cell cycle showing that it is cytostatic and increased apoptotic cell population in 48 hours treated CMT cells showing that pablociclib has cytostatic effect on CMT cells as well.

After performing the experiments on a larger number of CMT specimens and on suitable CMT cell lines, palbociclib can be suggested as a promising drug for the treatment of CMTs.

Conclusion

Despite preliminary, the results of this study indicate that CDK4/6 inhibition could be a valuable approach to treat CMTs. As first evidence, these results obviously need to be confirmed in a larger panel of cell lines and on different histotypes of CMTs.

However, this work has demonstrated that, similarly to HBC, deregulation of pRb family of proteins is a feature of CMTs and that it can be rescued by CDK4/6 inhibition. This study has also demonstrated that the palbociclib works on canine CDK4/6 in a specific manner like it does for the human isoforms.

In conclusion, this study gets the foundation for further investigation of the therapeutic potential of CDK4/6 inhibition for CMTs.

References

1. Manuscript A, Today CO. NIH Public Access. 2008;37(6):1-10.
2. Sultan F, Ganaie BA. Comparative oncology : Integrating human and veterinary medicine. 2018;8:25-34.
3. Gray M, Meehan J, Martínez-Pérez C, et al. Naturally-Occurring Canine Mammary Tumors as a Translational Model for Human Breast Cancer. *Front Oncol*. 2020;10(April):1-17. doi:10.3389/fonc.2020.00617
4. Hernández IB, Kromhout JZ, Teske E, Hennink WE, Van SA. Theranostics Molecular targets for anticancer therapies in companion animals and humans : what can we learn from each other ? 2021;11(8). doi:10.7150/thno.55760
5. Uehara TYR. Microsurgical Injection of Transformation. *Biol Reprod*. 1976;470:467-470.
6. Valdivia G, Alonso-diez Á, Pérez-alenza D, Peña L. From Conventional to Precision Therapy in Canine Mammary Cancer : A Comprehensive Review. 2021;8(February):1-33. doi:10.3389/fvets.2021.623800
7. Incidence of mammary tumors in the canine population living in the Veneto region (Northeastern Italy)_ Risk factors and similarities to human breast cancer - ScienceDirect.
8. Burrai GP, Gabrieli A, Moccia V, et al. A Statistical Analysis of Risk Factors and Biological Behavior in Canine Mammary Tumors : A Multicenter Study. Published online 2020.
9. Reddy GM. Clinicopathological Features of Triple Negative Breast Carcinoma. *J Clin DIAGNOSTIC Res*. Published online 2017:3-6.

doi:10.7860/jcdr/2017/21452.9187

10. Goldschmidt MH, Peña L, Rasotto R, Zappulli V. Classification and grading of canine mammary tumors. *Vet Pathol*. 2011;48(1):117-131. doi:10.1177/0300985810393258
11. Rasotto R, Berlato D, Goldschmidt MH, Zappulli V. Prognostic Significance of Canine Mammary Tumor Histologic Subtypes : An Observational Cohort Study of 229 Cases. 2017;54(4):571-578. doi:10.1177/0300985817698208
12. Patel MP, Ghodasara DJ, Raval SH, Joshi BP. Incidence, Gross Morphology, Histopathology and Immunohistochemistry of Canine Mammary Tumors. *Indian J Vet Sci Biotechnol*. 2019;14(04). doi:10.21887/ijvsbt.14.4.11
13. Liu D, Xiong H, Ellis AE, et al. Molecular homology and difference between spontaneous canine mammary cancer and human breast cancer. *Cancer Res*. 2014;74(18):5045-5056. doi:10.1158/0008-5472.CAN-14-0392
14. Sørlie T, Perou CM, Tibshirani R, et al. Gene expression patterns of breast carcinomas distinguish tumor subclasses with clinical implications. *Proc Natl Acad Sci U S A*. 2001;98(19):10869-10874. doi:10.1073/pnas.191367098
15. Dai X, Li T, Bai Z, et al. Breast cancer intrinsic subtype classification, clinical use and future trends. *Am J Cancer Res*. 2015;5(10):2929-2943.
16. Sweeney C, Bernard PS, Factor RE, et al. Intrinsic subtypes from PAM50 gene expression assay in a population-based breast cancer cohort: Differences by age, race, and tumor characteristics. *Cancer Epidemiol Biomarkers Prev*. 2014;23(5):714-724. doi:10.1158/1055-

9965.EPI-13-1023

17. Raj-Kumar PK, Liu J, Hooke JA, et al. PCA-PAM50 improves consistency between breast cancer intrinsic and clinical subtyping reclassifying a subset of luminal A tumors as luminal B. *Sci Rep*. 2019;9(1):1-13. doi:10.1038/s41598-019-44339-4
18. Herschkowitz JI, Simin K, Weigman VJ, et al. Identification of conserved gene expression features between murine mammary carcinoma models and human breast tumors. *Genome Biol*. 2007;8(5):1-17. doi:10.1186/gb-2007-8-5-r76
19. Prat A, Parker JS, Karginova O, et al. Phenotypic and molecular characterization of the claudin-low intrinsic subtype of breast cancer. Published online 2010.
20. Pareja F, Geyer FC, Marchiò C, Burke KA, Weigelt B, Reis-filho JS. Triple-negative breast cancer : the importance of molecular and histologic subtyping , and recognition of low-grade variants. 2016;7(July):1-11. doi:10.1038/npjbcancer.2016.36
21. Prat A, Adamo B, Cheang MCU, Anders CK, Carey LA, Perou CM. Molecular Characterization of Basal-Like and Non-Basal-Like Triple-Negative Breast Cancer. *Oncologist*. 2013;18(2):123-133. doi:10.1634/theoncologist.2012-0397
22. Abadie J, Nguyen F, Loussouarn D, et al. Canine invasive mammary carcinomas as models of human breast cancer. Part 2: immunophenotypes and prognostic significance. *Breast Cancer Res Treat*. 2018;167(2):459-468. doi:10.1007/s10549-017-4542-8
23. Im KS, Kim NH, Lim HY, Kim HW, Shin JI, Sur JH. Analysis of a New Histological and Molecular-Based Classification of Canine Mammary Neoplasia. *Vet Pathol*. 2014;51(3):549-559.

doi:10.1177/0300985813498780

24. Yadav S, Couch FJ. Germline Genetic Testing for Breast Cancer Risk: The Past, Present, and Future. *Am Soc Clin Oncol Educ B*. 2019;(39):61-74. doi:10.1200/edbk_238987
25. Hahnen E, Hauke J, Engel C, Neidhardt G, Rhiem K, Schmutzler RK. Germline Mutations in Triple-Negative Breast Cancer. *Breast Care*. 2017;12(1):15-19. doi:10.1159/000455999
26. Engel C, Rhiem K, Hahnen E, et al. Prevalence of pathogenic BRCA1/2 germline mutations among 802 women with unilateral triple-negative breast cancer without family cancer history. *BMC Cancer*. 2018;18(1):4-9. doi:10.1186/s12885-018-4029-y
27. Shi Y, Jin J, Ji W, Guan X. Therapeutic landscape in mutational triple negative breast cancer. *Mol Cancer*. 2018;17(1):1-11. doi:10.1186/s12943-018-0850-9
28. Shah Sohrab P., Roth Andrew, Goya Rodrigo, Oloumi Arusha HG, Zhao Y, Turashvili G, et al. The clonal and mutational evolution spectrum of primary triple negative breast cancers. *Nature*. 2013;486(7403):1-13. doi:10.1038/nature10933.The
29. Brough R, Gulati A, Haider S, et al. Identification of highly penetrant Rb-related synthetic lethal interactions in triple negative breast cancer. *Oncogene*. 2018;37(43):5701-5718. doi:10.1038/s41388-018-0368-z
30. Foley SA, Castell A, Kavanagh E, et al. MYC as a therapeutic target for the treatment of triple-negative breast cancer. *J Clin Oncol*. 2019;37(15_suppl):e12550-e12550. doi:10.1200/jco.2019.37.15_suppl.e12550
31. Andre F, Job B, Dessen P, et al. Molecular characterization of breast cancer with high-resolution oligonucleotide comparative genomic

hybridization array. *Clin Cancer Res*. 2009;15(2):441-451. doi:10.1158/1078-0432.CCR-08-1791

32. Laé M, Fréneaux P, Sastre-Garau X, Chouchane O, Sigal-Zafrani B, Vincent-Salomon A. Secretory breast carcinomas with ETV6-NTRK3 fusion gene belong to the basal-like carcinoma spectrum. *Mod Pathol*. 2009;22(2):291-298. doi:10.1038/modpathol.2008.184
33. Poling JS, Yonescu R, Subhawong AP, et al. MYB Labeling by Immunohistochemistry is More Sensitive and Specific for Breast Adenoid Cystic Carcinoma than MYB Labeling by FISH. *Am J Surg Pathol*. 2017;41(7):973-979. doi:10.1097/PAS.0000000000000878
34. Li Z, Zhang X, Hou C, Zhou Y. Comprehensive identification and characterization of somatic copy number alterations in triple - negative breast cancer. Published online 2019:1-9. doi:10.3892/ijo.2019.4950
35. Ha G, Roth A, Lai D, et al. Integrative analysis of genome-wide loss of heterozygosity and monoallelic expression at nucleotide resolution reveals disrupted pathways in triple-negative breast cancer. 2014;(May 2012). doi:10.1101/gr.137570.112
36. Kanwal R, Gupta S. Epigenetic modifications in cancer. *Clin Genet*. 2012;81(4):303-311. doi:10.1111/j.1399-0004.2011.01809.x
37. Sharma P, Stecklein SR, Kimler BF, et al. The prognostic value of BRCA1 promoter methylation in early stage triple negative breast cancer. *J Cancer Ther Res*. Published online 2014. doi:10.7243/2049-7962-3-2
38. Lips EH, Mulder L, Oonk A, et al. Triple-negative breast cancer: BRCAness and concordance of clinical features with BRCA1-mutation carriers. *Br J Cancer*. 2013;108(10):2172-2177. doi:10.1038/bjc.2013.144

39. Temian DC, Pop LA, Irimie AI, Berindan-neagoe I. Breast Cancer The Epigenetics of Triple-Negative and Basal-Like Breast Cancer : Current Knowledge. 2018;21(3):233-243.
40. Mora J, Alaminos M, De Torres C, et al. Comprehensive analysis of the 9p21 region in neuroblastoma suggests a role for genes mapping to 9p21-23 in the biology of favourable stage 4 tumours. *Br J Cancer*. 2004;91(6):1112-1118. doi:10.1038/sj.bjc.6602094
41. Pacifico A, Leone G. Role of p53 and CDKN2A inactivation in human squamous cell carcinomas. *J Biomed Biotechnol*. 2007;2007:1-5. doi:10.1155/2007/43418
42. Agarwal P, Lutful Kabir FM, DeInnocentes P, Curtis R. Tumor Suppressor Gene p16/INK4A/CDKN2A and Its Role in Cell Cycle Exit, Differentiation, and Determination of Cell Fate. *Tumor Suppressor Genes*. Published online 2012. doi:10.5772/27882
43. Kabir FML, Alvarez CE, Bird RC. Canine Mammary Carcinomas : A Comparative Analysis of Altered Gene Expression. 2016;(June 2015). doi:10.3390/vetsci3010001
44. Kaszak I, Ruszczak A, Kanafa S, Kacprzak K, Król M, Jurka P. Current biomarkers of canine mammary tumors. *Acta Vet Scand*. 2018;60(1):1-13. doi:10.1186/s13028-018-0417-1
45. Schiffman JD, Breen M. Comparative oncology: What dogs and other species can teach us about humans with cancer. *Philos Trans R Soc B Biol Sci*. 2015;370(1673). doi:10.1098/rstb.2014.0231
46. Soysal SD, Tzankov A, Muenst SE. Role of the Tumor Microenvironment in Breast Cancer. *Pathobiology*. 2015;82(3-4):142-152. doi:10.1159/000430499
47. Amini P, Ettlin J, Opitz L, Clementi E, Malbon A, Markkanen E. An

optimised protocol for isolation of RNA from small sections of laser-capture microdissected FFPE tissue amenable for next-generation sequencing. *BMC Mol Biol*. 2017;18(1):1-11. doi:10.1186/s12867-017-0099-7

48. Amini P, Nassiri S, Ettlin J, Malbon A, Markkanen E. Next-generation RNA sequencing of FFPE subsections reveals highly conserved stromal reprogramming between canine and human mammary carcinoma. *DMM Dis Model Mech*. 2019;12(8). doi:10.1242/dmm.040444
49. Markkanen E. Know Thy Model: Charting Molecular Homology in Stromal Reprogramming Between Canine and Human Mammary Tumors. *Front Cell Dev Biol*. 2019;7(December):1-12. doi:10.3389/fcell.2019.00348
50. Amini P, Nassiri S, Malbon A, Markkanen E. Differential stromal reprogramming in benign and malignant naturally occurring canine mammary tumours identifies disease-modulating stromal components. *Sci Rep*. 2020;10(1):1-13. doi:10.1038/s41598-020-62354-8
51. Maruvada P, Wang W, Wagner PD, Srivastava S. Biomarkers in molecular medicine: cancer detection and diagnosis. *Biotechniques*. Published online 2005. doi:10.2144/05384su04
52. Vivanco M d. M. Biomarkers in breast cancer. *Methods Mol Biol*. 2010;593:137-156. doi:10.2298/jmh0604355f
53. Carroll JS. Eje prize 2016: Mechanisms of oestrogen receptor (ER) gene regulation in breast cancer. *Eur J Endocrinol*. 2016;175(1):R41-R49. doi:10.1530/EJE-16-0124
54. Tang Z-R, Zhang R, Lian Z-X, Deng S-L, Yu K. Estrogen-Receptor Expression and Function in Female Reproductive Disease. *Cells*.

2019;8(10):1123. doi:10.3390/cells8101123

55. Hua H, Zhang H, Kong Q, Jiang Y. Mechanisms for estrogen receptor expression in human cancer 11 Medical and Health Sciences 1112 Oncology and Carcinogenesis 06 Biological Sciences 0604 Genetics. *Exp Hematol Oncol*. 2018;7(1):1-11. doi:10.1186/s40164-018-0116-7
56. Lim E, Palmieri C, Tilley WD. Renewed interest in the progesterone receptor in breast cancer. *Br J Cancer*. 2016;115(8):909-911. doi:10.1038/bjc.2016.303
57. Gown AM. Current issues in ER and HER2 testing by IHC in breast cancer. *Mod Pathol*. 2008;21:S8-S15. doi:10.1038/modpathol.2008.34
58. Allred DC. Issues and updates: Evaluating estrogen receptor-α, progesterone receptor, and HER2 in breast cancer. *Mod Pathol*. 2010;23(SUPPL. 2):52-59. doi:10.1038/modpathol.2010.55
59. Hammond MEH, Hayes DF, Dowsett M, et al. American society of clinical oncology/college of american pathologists guideline recommendations for immunohistochemical testing of estrogen and progesterone receptors in breast cancer. *J Clin Oncol*. 2010;28(16):2784-2795. doi:10.1200/JCO.2009.25.6529
60. Stocker A, Hilbers ML, Gauthier C, et al. HER2/CEP17 Ratios and Clinical Outcome in HER2-Positive Early Breast Cancer Undergoing Trastuzumab-Containing Therapy. *PLoS One*. 2016;11(7):e0159176. doi:10.1371/journal.pone.0159176
61. Maria Badowska-Kozakiewicz A, Piotr Budzik M. Triple-Negative Breast Cancer: Expression of Hypoxia-Inducible Factor 1α in Triple-Negative Breast Cancer with Metastasis to Lymph Nodes. *Breast Cancer Surg*. 2018;(November). doi:10.5772/intechopen.75354
62. Wang RX, Chen S, Jin X, Shao ZM. Value of Ki-67 expression in

triple-negative breast cancer before and after neoadjuvant chemotherapy with weekly paclitaxel plus carboplatin. *Sci Rep*. 2016;6(May):1-8. doi:10.1038/srep30091

63. Sobecki M, Mrouj K, Camasses A, et al. The cell proliferation antigen Ki-67 organises heterochromatin. *Elife*. 2016;5(MARCH2016):1-33. doi:10.7554/eLife.13722
64. Lyu H, Han A, Polsdofer E, Liu S, Liu B. Understanding the biology of HER3 receptor as a therapeutic target in human cancer. *Acta Pharm Sin B*. 2018;8(4):503-510. doi:10.1016/j.apsb.2018.05.010
65. Huang Q, Li S, Zhang L, et al. CAPE-PnO2 inhibited the growth and metastasis of triple-negative breast cancer via the EGFR/STAT3/AkT/E-cadherin signaling pathway. *Front Oncol*. 2019;9(JUN):1-14. doi:10.3389/fonc.2019.00461
66. Schweizer J, Bowden PE, Coulombe PA, et al. New consensus nomenclature for mammalian keratins. *J Cell Biol*. 2006;174(2):169-174. doi:10.1083/jcb.200603161
67. Moll R, Franke WW, Schiller DL, Geiger B, Krepler R. The catalog of human cytokeratins: Patterns of expression in normal epithelia, tumors and cultured cells. *Cell*. 1982;31(1):11-24. doi:10.1016/0092-8674(82)90400-7
68. Laakso M, Loman N, Borg Å, Isola J. Cytokeratin 5/14-positive breast cancer: True basal phenotype confined to BRCA1 tumors. *Mod Pathol*. 2005;18(10):1321-1328. doi:10.1038/modpathol.3800456
69. Hashmi AA, Naz S, Hashmi SK, et al. Cytokeratin 5/6 and cytokeratin 8/18 expression in triple negative breast cancers: Clinicopathologic significance in South-Asian population. *BMC Res Notes*. 2018;11(1):1-8. doi:10.1186/s13104-018-3477-4

70. Babaei A, by Dove Press published. DDDT-89114-receptor-tyrosine-kinase--c-kit--inhibitors--a-therapeutic-t. Published online 2016:2443-2459. doi:10.2147/DDDT.S89114
71. Janostiak R, Vyas M, Cicek AF, Wajapeyee N, Harigopal M. Loss of c-KIT expression in breast cancer correlates with malignant transformation of breast epithelium and is mediated by KIT gene promoter DNA hypermethylation. *Exp Mol Pathol*. 2018;105(1):41-49. doi:10.1016/j.yexmp.2018.05.011
72. Morales JC, Li L, Fattah FJ, et al. Review of poly (ADP-ribose) polymerase (PARP) mechanisms of action and rationale for targeting in cancer and other diseases. *Crit Rev Eukaryot Gene Expr*. 2014;24(1):15-28. doi:10.1615/CritRevEukaryotGeneExpr.2013006875
73. Amé JC, Spenlehauer C, De Murcia G. The PARP superfamily. *BioEssays*. 2004;26(8):882-893. doi:10.1002/bies.20085
74. Henning RJ, Bourgeois M, Harbison RD. Poly(ADP-ribose) Polymerase (PARP) and PARP Inhibitors: Mechanisms of Action and Role in Cardiovascular Disorders. *Cardiovasc Toxicol*. 2018;18(6):493-506. doi:10.1007/s12012-018-9462-2
75. Luo J, Jin J, Yang F, et al. The correlation between PARP1 and BRCA1 in AR positive triple-negative breast cancer. *Int J Biol Sci*. 2016;12(12):1500-1510. doi:10.7150/ijbs.16176
76. Tan ME, Li J, Xu HE, Melcher K, Yong EL. Androgen receptor: Structure, role in prostate cancer and drug discovery. *Acta Pharmacol Sin*. 2015;36(1):3-23. doi:10.1038/aps.2014.18
77. Gerratana L, Basile D, Buono G, et al. Androgen receptor in triple negative breast cancer: A potential target for the targetless subtype.

Cancer Treat Rev. 2018;68(April):102-110. doi:10.1016/j.ctrv.2018.06.005

78. Bhattarai S, Klimov S, Mittal K, et al. Prognostic role of androgen receptor in triple negative breast cancer: A multi-institutional study. *Cancers (Basel)*. 2019;11(7):1-9. doi:10.3390/cancers11070995
79. Kurozumi S, Inoue K, Matsumoto H, et al. Clinicopathological values of PD-L1 expression in HER2-positive breast cancer. *Sci Rep*. 2019;9(1):1-8. doi:10.1038/s41598-019-52944-6
80. Cyprian FS, Akhtar S, Gatalica Z, Vranic S. Targeted immunotherapy with a checkpoint inhibitor in combination with chemotherapy: A new clinical paradigm in the treatment of triple-negative breast cancer. *Bosn J Basic Med Sci*. 2019;19(3):227-233. doi:10.17305/bjbms.2019.4204
81. Hwang SY, Park S, Kwon Y. Recent therapeutic trends and promising targets in triple negative breast cancer. *Pharmacol Ther*. 2019;199:30-57. doi:10.1016/j.pharmthera.2019.02.006
82. Horne HN, Oh H, Sherman ME, et al. E-cadherin breast tumor expression, risk factors and survival: Pooled analysis of 5,933 cases from 12 studies in the Breast Cancer Association Consortium. *Sci Rep*. 2018;8(1):1-11. doi:10.1038/s41598-018-23733-4
83. Ginter PS, D'Alfonso TM. Current concepts in diagnosis, molecular features, and management of Lobular carcinoma in situ of the breast with a discussion of morphologic variants. *Arch Pathol Lab Med*. 2017;141(12):1668-1678. doi:10.5858/arpa.2016-0421-RA
84. Kashiwagi S, Yashiro M, Takashima T, et al. Significance of E-cadherin expression in triple-negative breast cancer. *Br J Cancer*. 2010;103(2):249-255. doi:10.1038/sj.bjc.6605735

85. Chen H, Liu H, Qing G. Targeting oncogenic Myc as a strategy for cancer treatment. *Signal Transduct Target Ther*. 2018;3(1):1-7. doi:10.1038/s41392-018-0008-7

86. Shen L, O'Shea JM, Kaadige MR, et al. Metabolic reprogramming in triple-negative breast cancer through Myc suppression of TXNIP. *Proc Natl Acad Sci U S A*. 2015;112(17):5425-5430. doi:10.1073/pnas.1501555112

87. Shao Y, Sun X, He Y, Liu C, Liu H. Elevated levels of serum tumor markers CEA and CA15-3 are prognostic parameters for different molecular subtypes of breast cancer. *PLoS One*. 2015;10(7):1-11. doi:10.1371/journal.pone.0133830

88. Wu JT. Expression of monoclonal antibody-defined tumor markers in four carcinomas. *Ann Clin Lab Sci*. 1989;19(1):17-26.

89. No JI, Yang JY, Hyun HJ, Yeon CS, Choi HJ. Factors associated with serum levels of carcinoembryonic antigen in healthy non-smokers. *Korean J Fam Med*. 2013;34(6):413-419. doi:10.4082/kjfm.2013.34.6.413

90. Liu H. Carcinoembryonic antigen is potential prognostic factor for patients with triple negative breast cancer. *Biomed Res*. 2017;28(15):6615-6618.

91. Manuali E, De Giuseppe A, Feliziani F, et al. CA 15-3 cell lines and tissue expression in canine mammary cancer and the correlation between serum levels and tumour histological grade. *BMC Vet Res*. 2012;8:86. doi:10.1186/1746-6148-8-86

92. Gardner HL, Fenger JM, London CA. Dogs as a Model for Cancer. *Annu Rev Anim Biosci*. Published online 2016. doi:10.1146/annurev-animal-022114-110911

93. How Many Chromosomes Do Dogs Have and What They Mean - Canine Campus Dog Daycare & Boarding.
94. Synchronization of Cultured Cells to G1, S, G2, and M Phases by Double Thymidine Block _ SpringerLink.
95. Activity B, Galderisi U. Different Stages of Quiescence , Senescence , and Cell Stress Identified by Molecular Algorithm Based on the Expression of. Published online 2021.
96. Waf C. The Role of Cell Cycle Regulators in Cell Survival — Dual Functions of Cyclin-Dependent. Published online 2020:1-14.
97. Signaling C. Regulation of Cell Cycle Progression by Growth Factor-Induced. Published online 2021.
98. Id KP, Lieberman K, Id NT, Id MO, Id FRC. *Control of Division in Chlamydomonas by Cyclin B / CDKB1 and the Anaphase-Promoting Complex*.; 2022. doi:10.1371/journal.pgen.1009997
99. Colas P. Cyclin-dependent kinases and rare developmental disorders. Published online 2020:1-14.
100. Quandt E, Ribeiro MPC, Clotet J. Atypical cyclins : the extended family portrait. *Cell Mol Life Sci*. 2020;(0123456789). doi:10.1007/s00018-019-03262-7
101. Mombach JCM, Bugs CA, Chaouiya C. Modelling the onset of senescence at the G1 / S cell cycle checkpoint. 2014;15(Suppl 7):1-11.
102. Schettini F, Santo I De, Rea CG, et al. CDK 4 / 6 Inhibitors as Single Agent in Advanced Solid Tumors. 2018;8(December):1-12. doi:10.3389/fonc.2018.00608
103. Robbins & Cotran Pathologic Basis of Disease - 10th Edition.
104. Verdugo-sivianes EM. Role of the Holoenzyme PP1-SPN in the Dephosphorylation of the RB Family of Tumor Suppressors During

Cell Cycle. Published online 2021.

105. Henley SA, Dick FA. The retinoblastoma family of proteins and their regulatory functions in the mammalian cell division cycle. *Cell Div*. Published online 2012. doi:10.1186/1747-1028-7-10
106. Piezzo M, Cocco S, Caputo R, et al. Targeting Cell Cycle in Breast Cancer : CDK4 / 6 Inhibitors.
107. Wagner V, Gil J. Europe PMC Funders Group Senescence as a therapeutically relevant response to CDK4 / 6 inhibitors. 2021;39(29):5165-5176. doi:10.1038/s41388-020-1354-9.Senescence
108. Bosco EE, Wang Y, Xu H, et al. The retinoblastoma tumor suppressor modifies the therapeutic response of breast cancer. *J Clin Invest*. 2007;117(1):218-228. doi:10.1172/JCI28803
109. Ewens KG, Bhatti TR, Moran KA, et al. inactivation in MYCN - - amplified retinoblastoma. Published online 2017:619-630. doi:10.1002/cam4.1010
110. Knudsen ES, Nambiar R, Rosario SR, Smiraglia DJ, Goodrich DW, Witkiewicz AK. suppressor pathway. *Commun Biol*. (2020):1-12. doi:10.1038/s42003-020-0873-9
111. Mandigo AC, Tomlins SA, Kelly WK, Knudsen KE. Relevance of pRB Loss in Human Malignancies. Published online 2022:255-264. doi:10.1158/1078-0432.CCR-21-1565
112. Knudsen ES, Zacksenhaus E. The vulnerability of RB loss in breast cancer : Targeting a void in cell cycle control. 2018;9(57):30940-30941.
113. Leser C, Reiner A, Dorffner G, et al. Altered Expression of RB and pRB in Tissue Arrays of Primary Breast Cancers and Matched Axillary Lymph Node Metastases. 2022;2022:3-8.

114. RB1 in cancer_ Different mechanisms of RB1 inactivation and alterations of pRb pathway in tumorigenesis - Di Fiore - 2013 - Journal of Cellular Physiology - Wiley Online Library.
115. Wu T, Wu L. The Role and Clinical Implications of the Retinoblastoma (RB) -E2F Pathway in Gastric Cancer. 2021;11(May):1-15. doi:10.3389/fonc.2021.655630
116. Thomas R, Wang HJ, Tsai P, et al. Europe PMC Funders Group Influence of genetic background on tumor karyotypes : evidence for breed-associated cytogenetic aberrations in canine appendicular osteosarcoma. 2013;17(3):612-625. doi:10.1007/s10577-009-9028-z.Influence
117. RB1 RB transcriptional corepressor 1 [Canis lupus familiaris (dog)] - Gene - NCBI.
118. Hospital X, Military F, Province S, et al. Epidemiology and 1 1 gene of retinoblastoma. 2011;4(1):103-109. doi:10.3980/j.issn.2222-3959.2011.01.24
119. Molecular cloning, chromosomal mapping, and expression of the cDNA for p107, a retinoblastoma gene product-related protein - ScienceDirect.
120. Andrilli GD, Masciullo V, Bagella L, et al. Frequent Loss of pRb2 / p130 in Human Ovarian Carcinoma. 2004;10(215):3098-3103.
121. Masciullo V, Valdivieso P, Amadio G, Santoro A, Scambia G, Zannoni GF. Role of Retinoblastoma Protein Family (Rb / p105 and Rb2 / p130) Expression in the Histopathological Classification of Borderline Ovarian Tumors. 2020;7(November):1-9. doi:10.3389/fmed.2020.596226
122. Retinoblastoma family genes - PMC.

123. Dick FA. Structure-function analysis of the retinoblastoma tumor suppressor protein – is the whole a sum of its parts ? 2007;15:1-15. doi:10.1186/1747-1028-2-26
124. Wikenheiser-brokamp KA. Rb family proteins differentially regulate distinct cell lineages during epithelial development. Published online 2004:4299-4310. doi:10.1242/dev.01232
125. Mäkelä J, Toppari J. Retinoblastoma-E2F Transcription Factor Interplay Is Essential for Testicular Development and Male Fertility. 2022;13(May):1-15. doi:10.3389/fendo.2022.903684
126. Xie D, Pei Q, Li J, Wan X, Ye T. Emerging Role of E2F Family in Cancer Stem Cells. 2021;11(August):1-12. doi:10.3389/fonc.2021.723137
127. Cicchillitti L, Fasanaro P, Biglioli P, Capogrossi MC, Martelli F. Oxidative Stress Induces Protein Phosphatase 2A-dependent Dephosphorylation of the Pocket Proteins pRb , p107 , and p130 *. *J Biol Chem*. 2003;278(21):19509-19517. doi:10.1074/jbc.M300511200
128. Henley SA, Dick FA. The retinoblastoma family of proteins and their regulatory functions in the mammalian cell division cycle. *Cell Div*. 2012;7(1):10. doi:10.1186/1747-1028-7-10
129. Structure of the retinoblastoma tumour-suppressor pocket domain bound to a peptide from HPV E7 _ Nature.
130. Hu Q, Dyson N, Harlow E. The regions of the retinoblastoma protein needed for binding to adenovirus E1A or SV40 large T antigen are common sites for mutations. 1990;9(4).
131. p107 and p130_ Versatile Proteins with Interesting Pockets - ScienceDirect.
132. Litovchick L, Chestukhin A, Decaprio JA. Glycogen Synthase Kinase

3 Phosphorylates RBL2 / p130 during Quiescence. 2004;24(20):8970-8980. doi:10.1128/MCB.24.20.8970

133. Lees JA, Saito M, Vidal M, et al. The Retinoblastoma Protein Binds to a Family of E2F Transcription Factors. 1993;13(12):7813-7825.
134. Takahashi Y, Rayman JB, Dynlacht BD. Analysis of promoter binding by the E2F and pRB families in vivo : distinct E2F proteins mediate activation and repression. Published online 2000:804-816.
135. Wells J, Boyd KE, Fry CJ, Bartley SM, Farnham PJ. Target Gene Specificity of E2F and Pocket Protein Family Members in Living Cells. 2000;20(16):5797-5807.
136. Ezhevsky SA, Ho A, Becker-hapak M, Davis PK, Dowdy SF. Differential Regulation of Retinoblastoma Tumor Suppressor Protein by G 1 Cyclin-Dependent Kinase Complexes In Vivo. 2001;21(14):4773-4784. doi:10.1128/MCB.21.14.4773
137. Control of pRB phosphorylation - ScienceDirect.
138. Lundberg AS. Functional Inactivation of the Retinoblastoma Protein Requires Sequential Modification by at Least Two Distinct Cyclin-cdk Complexes. 1998;18(2):753-761.
139. Knudsen KE, Booth D, Naderi S, et al. RB-Dependent S-Phase Response to DNA Damage. 2000;20(20):7751-7763.
140. Cito L, Pentimalli F, Forte I, Mattioli E, Giordano A. Rb family proteins in gastric cancer (Review). Published online 2010:1411-1418. doi:10.3892/or
141. MacDonald JI, Dick FA. Posttranslational modifications of the retinoblastoma tumor suppressor protein as determinants of function. *Genes and Cancer*. Published online 2012. doi:10.1177/1947601912473305

142. Markham D, Munro S, Soloway J, Connor DPO, Thangue NB La, Hospital JR. scientific report. 2006;7(2). doi:10.1038/sj.embor.7400591
143. Role of the RB1 family in stabilizing histone methylation at constitutive heterochromatin - PubMed.
144. Durfee T, Becherer K, Chen P, et al. The retinoblastoma protein associates with the protein phosphatase type 1 catalytic subunit. Published online 1993:555-569.
145. Garriga J, Jayaraman AL, Limón A, et al. es Bio Do No t D ist r. 2004;4101. doi:10.4161/cc.3.10.1183
146. Manuscript A. NIH Public Access. 2013;19(6):658-662. doi:10.1016/j.ceb.2007.10.003.E2F-associated
147. Chicas A, Wang X, Zhang C, et al. NIH Public Access. 2010;17(4):376-387. doi:10.1016/j.ccr.2010.01.023.Dissecting
148. Flores M, Goodrich DW. Retinoblastoma Protein Paralogs and Tumor Suppression. 2022;13(March):1-17. doi:10.3389/fgene.2022.818719
149. Ventura E, Iannuzzi CA, Pentimalli F, Giordano A, Morrione A. RBL1 / p107 Expression Levels Are Modulated by Multiple Signaling Pathways. Published online 2021.
150. Schade AE, Fischer M, DeCaprio JA. RB, p130 and p107 differentially repress G1/S and G2/M genes after p53 activation. *Nucleic Acids Res*. Published online 2019. doi:10.1093/nar/gkz961
151. Zhang M, Zhang L, Hei R, et al. Review Article CDK inhibitors in cancer therapy , an overview of recent development. 2021;11(5):1913-1935.
152. Malumbres M, Harlow E, Hunt T, et al. Cyclin-dependent kinases : a family portrait. 2010;11(11):1275-1276. doi:10.1038/ncb1109-

1275.Cyclin-dependent

153. Rev N, Discov D. HHS Public Access. 2015;14(2):130-146. doi:10.1038/nrd4504.The
154. Elder K, Dale B. Assisted reproductive technology in farm animals. *Vitr Fertil*. 2009;(October):93-108. doi:10.1017/cbo9780511545146.007
155. Osman S, Mohammad E, Lidschreiber M, et al. The Cdk8 kinase module regulates interaction of the mediator complex with RNA polymerase II. *J Biol Chem*. 2021;296(14):100734. doi:10.1016/j.jbc.2021.100734
156. Kim YK, Bourgeois CF, Isel C, Churcher MJ, Karn J. Phosphorylation of the RNA Polymerase II Carboxyl-Terminal Domain by CDK9 Is Directly Responsible for Human Immunodeficiency Virus Type 1 Tat-Activated Transcriptional Elongation. 2002;22(13):4622-4637. doi:10.1128/MCB.22.13.4622
157. Ettl T, Schulz D, Bauer RJ. The Renaissance of Cyclin Dependent Kinase Inhibitors. Published online 2022.
158. Niu Y, Xu J, Sun T. Cyclin-dependent kinases 4/6 inhibitors in breast cancer: Current status, resistance, and combination strategies. *J Cancer*. 2019;10(22):5504-5517. doi:10.7150/jca.32628
159. Tripathy D, Bardia A, Sellers WR. HHS Public Access. 2018;23(13):3251-3262. doi:10.1158/1078-0432.CCR-16-3157.Ribociclib
160. George MA, Qureshi S, Omene C, Toppmeyer DL. Clinical and Pharmacologic Differences of CDK4 / 6 Inhibitors in Breast Cancer. 2021;11(July). doi:10.3389/fonc.2021.693104
161. Pack LR, Daigh LH, Chung M, Meyer T. Clinical CDK4/6 inhibitors

induce selective and immediate dissociation of p21 from cyclin D-CDK4 to inhibit CDK2. *Nat Commun*. (2021):1-12. doi:10.1038/s41467-021-23612-z

162. Rubin SM, Sage J, Skotheim JM. Review Integrating Old and New Paradigms of G1 / S Control. *Mol Cell*. 2020;80(2):183-192. doi:10.1016/j.molcel.2020.08.020
163. Watt AC, Goel S. Cellular mechanisms underlying response and resistance to CDK4 / 6 inhibitors in the treatment of hormone receptor - positive breast cancer. *Breast Cancer Res*. Published online 2022. doi:10.1186/s13058-022-01510-6
164. Wang B, Li R, Wu S, et al. Breast Cancer Resistance to Inhibitors : Intricacy of the Molecular Mechanisms. 2021;11(May):1-12. doi:10.3389/fonc.2021.651541
165. Strategies C. HHS Public Access. 2018;3(1):39-55. doi:10.1016/j.trecan.2016.11.006.The
166. Pernas S, Tolaney SM, Winer EP, Goel S. CDK4 / 6 inhibition in breast cancer : current practice and future directions. Published online 2018:1-15. doi:10.1177/1758835918786451
167. Contribution of gut microbiota and multiple organ failure in the pathogenesis of COVID-19 infection. 2020;(January).
168. Specific inhibition of cyclin-dependent kinase 4_6 by PD 0332991 and associated antitumor activity in human tumor xenografts - PubMed.
169. Demichele A, Clark AS, Tan KS, et al. CDK 4 / 6 Inhibitor Palbociclib (PD0332991) in Rb þ Advanced Breast Cancer : Phase II Activity , Safety , and Predictive Biomarker Assessment. :995-1001. doi:10.1158/1078-0432.CCR-14-2258
170. Determination of stable housekeeping genes, differentially regulated

target genes and sample integrity_ BestKeeper – Excel-based tool using pair-wise correlations _ SpringerLink.

171. Analysis of Relative Gene Expression Data Using Real-Time Quantitative PCR and the 2−ΔΔCT Method - ScienceDirect.
172. Clonogenic assay of cells in vitro _ Nature Protocols.
173. Liang C, Park AY, Guan J. In vitro scratch assay : a convenient and inexpensive method for analysis of cell migration in vitro. 2007;2(2):329-333. doi:10.1038/nprot.2007.30
174. Esumi H, Lu J, Kurashima Y, Hanaoka T. Antitumor activity of pyrvinium pamoate , salt , showing preferential cytotoxicity during glucose starvation. 2004;95(8):685-690.
175. Espérance SL, Bachvarova M, Tetu B, Mes-masson M, Bachvarov D. Global gene expression analysis of early response to chemotherapy treatment in ovarian cancer spheroids. 2008;21:1-21. doi:10.1186/1471-2164-9-99
176. Advantages & Disadvantages of Primary Cells in Animal Tissue Culture.
177. Colin L, Cristina T. HER2 / p53 ratios among canine mammary tumours and respective derived cell culture. 2022;53.
178. Yonemaru K, Sakai H, Murakami M, Kodama A, Mori T. The Significance of p53 and Retinoblastoma Pathways in Canine Hemangiosarcoma. Published online 2006.
179. Gau DM, Roy P. www.bio-protocol.org/e3586. 2020;10(08):1-9. doi:10.21769/BioProtoc.3586
180. Yakavets I, Francois A, Benoit A, Merlin JL, Bezdetnaya L, Vogin G. Advanced co - culture 3D breast cancer model for investigation of fibrosis induced by external stimuli : optimization study. *Sci Rep*.

Published online 2020:1-11. doi:10.1038/s41598-020-78087-7